

THE MILLIARCSECOND STRUCTURE OF HIGHLY VARIABLE RADIO SOURCES

ANN E. WEHRLE,¹ MARSHALL H. COHEN, AND STEPHEN C. UNWIN
 Owens Valley Radio Observatory, Mail Code 105-24, California Institute of Technology, Pasadena, CA 91125

HUGH D. ALLER AND MARGO F. ALLER
 Radio Astronomy Observatory, University of Michigan, Ann Arbor, MI 48109

AND

GEORGE NICOLSON
 Hartebeesthoek Radio Astronomy Observatory, P.O. Box 443, Krugersdorp 1740, South Africa
 Received 1990 December 12; accepted 1991 November 20

ABSTRACT

We define a new sample of core-dominated extragalactic sources: those whose flux density has exceeded 4.5 Jy at 8 GHz at any epoch. This Variable Source Sample has 41 members.

We have begun a program of VLBI studies of those members of the Variable Source Sample which are not otherwise being observed. In this paper we show first-epoch maps 12 of the 13 new objects. We discuss the morphologies and “scale lengths” (analogous to e -folding lengths) of sources in the complete Variable Source Sample to the extent these quantities are known, and compare them to the sources in the complete flux-limited sample of Pearson & Readhead (1988). We also discuss the ratio of X-ray to radio luminosities of sources in the Variable Source Sample.

Our principal results are the following:

1. The morphologies of the Variable Source Sample and Pearson-Readhead sources are similar.
2. We confirm the Pearson-Readhead result that the distribution of position angle differences between milli-arcsecond and arcsecond scales shows peaks at 0° and 90° .
3. In our VLBI images, the “scale lengths” of Variable Source Sample and Pearson-Readhead sources are all smaller than about 120 pc. Compact Steep Spectrum sources have the largest scale lengths. BL Lac objects have much smaller scale lengths.
4. BL Lac objects have significantly higher ratios of X-ray to radio luminosities than the quasars in the Variable Source Sample.

Subject headings: galaxies: active — galaxies: jets — galaxies: nuclei — quasars: general — radio continuum: galaxies

1. INTRODUCTION

This program was started in 1985 to take advantage of the large Block II VLBI Processor (built jointly by JPL and Caltech) that was beginning to come on line. This processor cross-correlates up to 16 Mark II (narrow band: 2 MHz) VHS video cassettes simultaneously. Thus data from 16 telescopes can be correlated in “real-time” (after tape shipment to the correlator), and up to 24 telescopes can be processed in 3 times “real-time” (O’Connor 1988, 1989). This represented a large increase in VLBI capability and allowed, for the first time, the analysis of VLBI snapshot experiments. Snapshots are routinely made at the VLA with 27 telescopes, and over the last few years have become more common in VLBI, with typically a dozen telescopes at 5 GHz. In the work described below we used 12 or 13 telescopes, and for most sources used three or four snapshots of duration 1 hr.

The snapshot possibility meant that large surveys could be undertaken with only modest requirements of observing time; but only strong sources could be observed, because of the narrow bandwidth. In 1985 fewer than half of the known core-dominated extragalactic sources stronger than 5 Jy at 8 GHz

had been mapped with VLBI, and we started a program to observe them, and seek superluminal motions.

We had two main scientific objectives:

1. To obtain a large body of data on superluminal sources, in order to study their statistics and test theories of beaming and unification. This would extend the scope of the complete VLBI surveys of Pearson & Readhead (1988, hereafter PR88) and Eckart et al. (1987), which cover only a small part of the sky but go to lower flux density.

2. To study how the superluminal motion, and the source morphology, depend on redshift. If the jet Lorentz factor $\gamma = (1 - v^2/c^2)^{-0.5}$ does not have a large spread, then a reduction in proper motion μ with redshift is expected. This has now been demonstrated through the “ $(\mu-z)$ ” diagram (Cohen et al. 1988), and it appears that this work will be useful in constraining both beaming theories and cosmological models.

To maximize the “yield” of superluminal sources in our sample, we chose a flux density cutoff of 4.5 Jy at 8 GHz, and selected objects which exceeded this limit at *any* epoch. Choosing objects in this way emphasizes variability and hence, we believe, favors inclusion of superluminal sources. At least nine of the 12 strongest sources in our sample have displayed superluminal motion (Cohen 1990).

In the next section we discuss the selection criteria, and present in Table 1 our sample of 41 objects which we call the

¹ Postal address and additional affiliation: Infrared Processing and Analysis Center, Mail Code 100-22, California Institute of Technology, Pasadena, CA 91125.

“Variable Source Sample.” Section 3 describes our VLBI observations of Variable Source Sample objects. About half of them are being studied under other VLBI programs, and we have undertaken observations of 15 of those remaining. Results for two have already been published: 0106+013 shows superluminal motion (Wehrle & Cohen 1989), and we derived a 6 cm upper limit to superluminal motion for CTA 102 (Wehrle, Cohen, & Unwin 1990a). A third object (3C 446) has now been observed at several epochs and the data are being analyzed. First-epoch images of the remaining 12 (as well as one other high-redshift object which does not meet the flux density criterion) are presented in § 4.

Section 5 discusses the VLBI source structures in relation to those of other VLBI surveys, and any arcsecond-scale structures seen with the VLA or with MERLIN. In § 6 we discuss the scale lengths of the Variable Source Sample sources and their relation to other properties. In § 7 we examine the ratio of X-ray to radio luminosities of the Variable Source Sample sources to study possible differences in the contribution of beamed inverse-Compton radiation in BL Lac objects and quasars. We consider the effects of orientation on the (apparent) source luminosities in § 8. Section 9 summarizes our principal results. Throughout this paper we use a Hubble constant $H_0 = 100 \text{ km s}^{-1} \text{ Mpc}^{-1}$ and $q_0 = 0.5$.

An early version of Table 1, with sources selected at 10.7 GHz, was presented by Wehrle, Cohen, & Unwin (1990b). The strongest 12 objects in the Variable Source Sample have been analyzed by Cohen (1990); nine of them are superluminal unless $H_0 > 150 \text{ km s}^{-1} \text{ Mpc}^{-1}$ and this implies that they radiate anisotropically.

2. SAMPLE SELECTION AND COMPLETENESS

We picked 8 GHz as the selection frequency to take advantage of the long runs of flux density monitoring at the University of Michigan Radio Astronomy Observatory, and the earlier variability studies at 8 GHz made by Dent and his collaborators. Also, both the VLA and the VLBA have 8 GHz as one of the primary observing frequencies, and for VLBI studies 8 GHz will soon replace 10.7 GHz, which has been more commonly used in the past.

We define $S_m(8)$ as the maximum value ever measured at 8 GHz for the flux density from the compact core of an extragalactic object. We picked objects with $S_m(8) \geq 4.5 \text{ Jy}$, mainly from the observations of UMRAO, but we also searched the literature for earlier observations and a few of them made the list. The UMRAO observations are on the flux density scale set by Baars et al. (1977), and we have not attempted to rescale the earlier observations to this scale. The longest runs of data are over 20 yr long, and a few short ones are only a few years long. Thus, the observations are inhomogeneous and incomplete, as discussed below.

Table 1 shows the 41 sources which have $S_m(8) \geq 4.5 \text{ Jy}$ and $\delta > -18^\circ$. Radio light curves from UMRAO are shown in Figure 1 for the objects we observed with VLBI. Many of these objects are strongly variable, and some (e.g., 3C 120) which have strong outbursts with a low duty cycle, and would not appear in a conventional flux-density limited sample. We did not exclude sources at low Galactic latitude. The flux density refers to the core only, so that extended objects like 3C 274, with weak cores, are not included. Column (3) gives the identification: Q = quasar, BL = BL Lac object, Gal = galaxy, and EF = empty field. Column (5) gives the galactic latitude; note that only four objects have $b < 10^\circ$. Columns (6) and (7) give

$S_m(8)$ and its epoch; column (8) gives the apparent transverse velocity. Column (9) gives an indication of the VLBI observations currently being made: 1, 2, and 3 refer to our observing sessions in 1986, 1987, and 1988, respectively (see § 3 below); “P/R” refers to the Pearson-Readhead survey, and an asterisk means that the source is being observed by other groups. Column (10) gives references for the velocity and the flux density.

The more customary definition of a flux-limited sample includes all those objects greater than a fixed value at some given epoch; or those greater than a fixed value the first time they are measured. In such a sample the individual sources would change as the epochs change because many sources are variable, but the statistical content of the sample is assumed to be independent of epoch. Our sample, on the other hand, has fixed objects but new ones are added as outbursts raise new sources above the flux cutoff. It tends to include sources which are on average weaker, and more variable, than those in a single-epoch sample.

The Variable Source Sample may well be incomplete because of source variability, especially near the flux cutoff, but this effect may be offset somewhat by the standard Malmquist bias. Apart from the possible incompleteness our sample is just as valid as one selected by ignoring the effects of variability. For example, V/V_m tests can be made as with any complete flux-limited sample. “Complete” VLBI samples include the surveys of Pearson & Readhead (1988), Hough & Readhead (1987, 1989), Zensus & Porcas (1987), and Eckart et al. (1987).

Separating the Variable Source Sample objects into four bins with the flux density ratios of 2:1 yields $N = 31, 6, 2,$ and 2 objects. Although the numbers are small, the $\log N/\log S_m$ slope is consistent with the value found for the normal 6 cm counts, which is -1.8 for strong, flat-spectrum objects (Condon 1988, see Fig. 15.6). Our sample is not seriously deficient at low flux levels. We presume that only a few sources have been missed because of variability or for other reasons, and doubt that any sources brighter than, say, 7 Jy have been missed.

We might also wonder if the list is underpopulated at low declinations, where there has been less study and monitoring. Binning into four bins of equal solid angle, north of $\delta = -18^\circ$, gives $N = 4, 12, 10,$ and 15 objects, starting at the North Pole. We seem to have a deficiency of high-declination sources; not of those with $\delta < 0$. This is partly due to obscuration and the lack of study near the Galactic plane; nearly one-fourth of the sky in the northern bin ($42.3^\circ < \delta < 90^\circ$) has $|b| < 10^\circ$. The UMRAO telescope has a northern declination limit of 80° and the NRAO² 300 foot telescope had a similar limit. Sources in the excluded region help make up the remaining deficit.

Some sources in the sample, such as 3C 84 and 3C 273, are famous because they are strong and have interesting structure, but others have been studied extensively because their high variability makes them intrinsically interesting, e.g., they are optically violent variables or BL Lac objects. Some of the ones which are particularly compact and bright have become important as calibration or reference objects for VLBI, in fields such as reference frames, spacecraft tracking and crustal dynamics.

A SIMBAD³ search through the literature since 1980 turned

² The National Radio Astronomy Observatory is operated by Associated Universities, Inc., under cooperative contract with the National Science Foundation.

³ The SIMBAD data retrieval system is a database of the Strasbourg, France, Astronomical Data Center.

TABLE 1
 THE VARIABLE SOURCE SAMPLE

NAME	ALT	ID	z	bII	Sm(8)	EPOCH	v/c	VLBI	REF
0106+013		Q	2.107	-49.3	5.5	73.4	8.2	1,3	1,2
0133+476	DA 55	Q	0.859	-14.3	5.6(a)	68.8		P/R	7
0234+285	CTD 20	Q	1.213	-28.5	5.6	88.7		3	3
0235+164		BL	0.94	-39.1	6.8	75.9		*	4
0316+413	3C 84	Gal	0.0172	-13.3	60.7	83.2	0.2	P/R, *	3, 5, 6
0336-019	CTA 26	Q	0.852	-42.5	4.7	72.2		2	1
0355+508	NRAO 150	EF		-1.6	12.8	77.5			4,22
0420-014		Q	0.915	-33.1	7.1	86.4		1	3
0430+052	3C 120	Gal	0.033	-27.4	15.2(a)	73.2	4.1	*	4,7
0458-020		Q	2.286	-25.3	4.6	89.8		3	3
0528+134		EF		-11.0	4.9	81.9			4,23
0538+498	3C 147	Q	0.545	10.3	5.3(a)	b	(1.3)	P/R, *	7,8
0552+398	DA 193	Q	2.365	7.3	7.3	89.6		2	3
0605-085		Q	0.87	-13.5	4.6	72.5		*	1
0607-157		Q	0.324	-16.2	6.3	85.6		*	3
0727-115		EF		3.2	6.5	85.8		3,21	
0735+178		BL	0.424	18.1	5.1	89.6	2.8	*	3,9,24
0851+202	OJ 287	BL	0.306	35.8	8.5	73.0	3.3	*	1,10
0923+392	4C 39.25	Q	0.699	46.2	11.8	73.0	3.5	P/R, *	1,11
1127-145		Q	1.187	43.6	6.9	68.2		3	4
1226+023	3C 273	Q	0.158	64.4	53.2	71.7	8.0	*	1,12
1253-055	3C 279	Q	0.538	57.1	19.2	68.2	9.2	*	4,13
1328+307	3C 286	Q	0.846	80.7	5.3(a)	b		*	7
1335-127	1334-127	Q	0.541	48.4	8.1	86.9		2	3
1510-089		Q	0.361	40.1	4.9	88.5		*	3
1633+382		Q	1.814	42.3	5.2	74.7		P/R	4
1641+399	3C 345	Q	0.595	40.9	15.0	82.1	9.5	P/R, *	3,14
1730-130	NRAO 530	Q	0.902	-10.8	7.7	87.3		*	3
1749+096	OT 081	BL	0.321	17.6	5.4	85.9		1,2	3
1828+487	3C 380	Q	0.691	23.5	5.7	72.5		P/R	1
1928+738		Q	0.302	23.5	4.6	89.0	7.0	P/R, *	3
2005+403		Q	1.736	4.3	8.0	75.5	2, *	4,15	
2121+053	OX 036	Q	1.878	-30.1	5.5	80.6		3	3
2134+004		Q	1.936	-35.6	13.4	68.5	(<.04)	*	4,16
2145+067		Q	0.990	-34.1	7.2	88.2		1	3
2200+420	BI Lac	BL	0.0695	-10.4	12.3	80.7	3.7	P/R, *	3,17
2201+315	4C 31.63	Q	0.297	-18.8	4.8	84.4			3
2223-052	3C 446	BL	1.404	-48.8	8.8	84.3	(3)	1,2,3	3,18
2230+114	CTA 102	Q	1.037	-38.6	4.8	81.3	<10.0	2,3	3,19
2251+158	3C 454.3	Q	0.859	-38.2	26.3	67.5	8.8	*	4,20
2345-167		Q	0.600	-71.9	4.5	72.9		2	1
2136+141 (c)	OX 161	Q	2.427	-27.4	1.4	N/A		3	3

a) Interpolated

b) Not variable

c) Not in Variable Source Sample

(1) Dent & Kapitzky 1976. (2) Wehrle, Cohen, & Unwin 1990a, b. (3) Aller et al. 1992, in preparation (data since ApJS paper). (4) Aller et al. 1985. (5) O'Dea, Dent, & Balonek 1984. (6) Marr et al. 1992, in preparation. (7) Andrew et al. 1978. (8) Alef et al. 1988. (9) Bááth 1984. (10) Roberts, Gabuzda, & Wardle 1987. (11) Schalinski et al. 1988. (12) Zensus et al. 1988. (13) Unwin et al. 1989. (14) Biretta et al. 1986. (15) Mutel & Lestrader 1990. (16) Pauliny-Toth et al. 1990. (17) Mutel et al. 1990. (18) Cohen M. H. et al. 1992, in preparation. (19) Wehrle & Cohen 1989. (20) Pauliny-Toth et al. 1987. (21) Torres & Wroblewski 1987. (22) Argue & Sullivan 1980. (23) Bregman et al. 1985. (24) Bregman et al. 1984.

up an average of 50 references per source. Some of these references are in Table 2. Centimeter-wavelength light curves from the monitoring program at the University of Michigan (Aller, Aller, & Hodge 1981; Aller et al. 1985) are in Figure 1, for the 16 objects we have observed. Most of them have also been monitored at millimeter wavelengths by Valtaoja et al. (1988), and by Edelson (1987) and Steppe et al. (1988). Additional observations at 8.2 mm have been reported by Moiseev et al. (1988). JPL groups have observed nearly all the objects with

two-station VLBI using the DSN antennas in Goldstone (USA), Madrid (Spain) and Tidbinbilla (Australia) (Wehrle, Morabito, & Preston 1984; Preston et al. 1985; Morabito et al. 1986).

3. OBSERVATIONS

Three observing sessions were conducted with the Global VLBI Array in June of 1986, 1987, and 1988 (Table 3). The

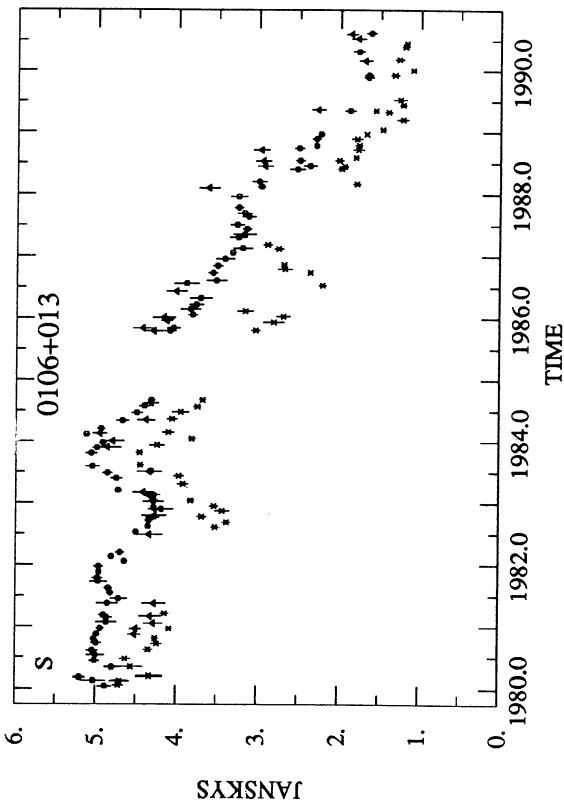


FIG. 1a

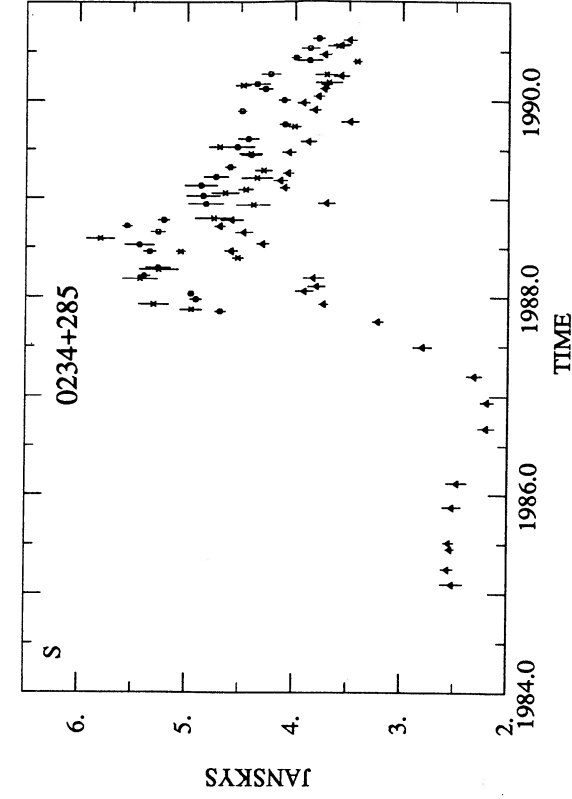


FIG. 1b

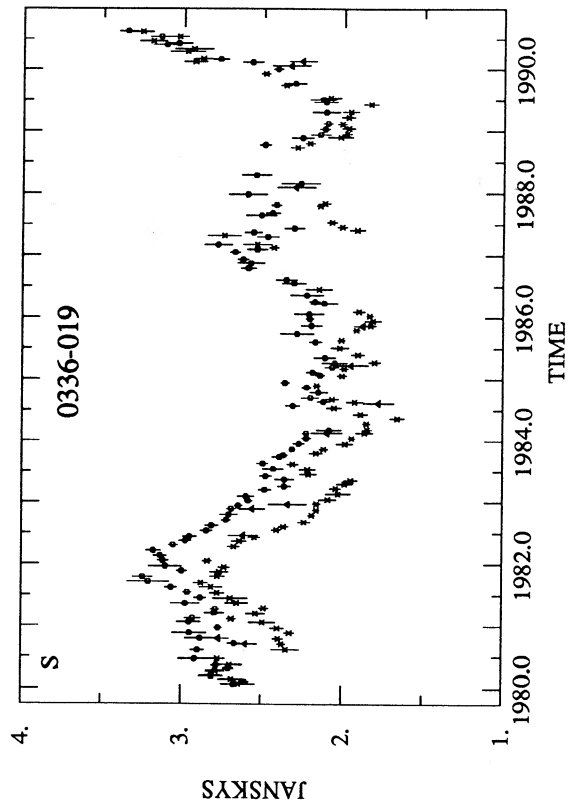


FIG. 1c

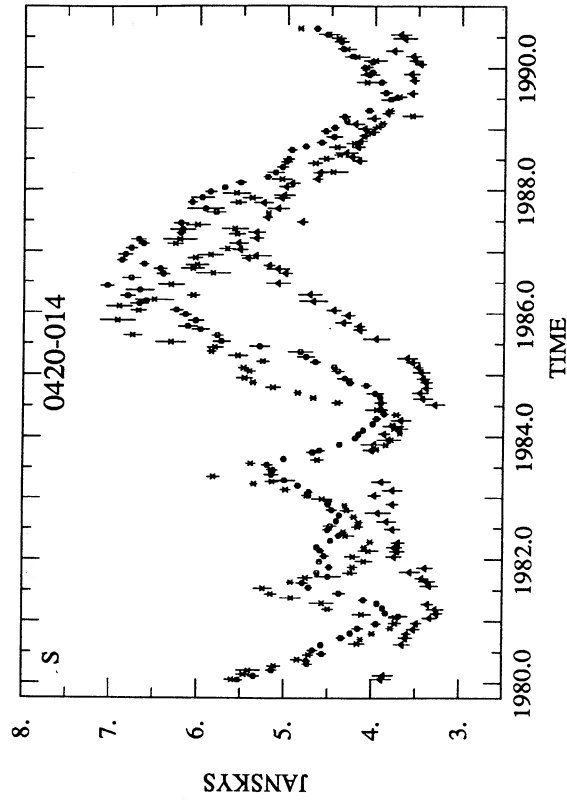


FIG. 1d

FIG. 1.—Radio flux density curves from the University of Michigan Radio Astronomy Observatory monitoring program. Data shown are monthly averages at three frequencies: 4.8 GHz (triangles), 8.0 GHz (circles), and 14.5 GHz (squares).

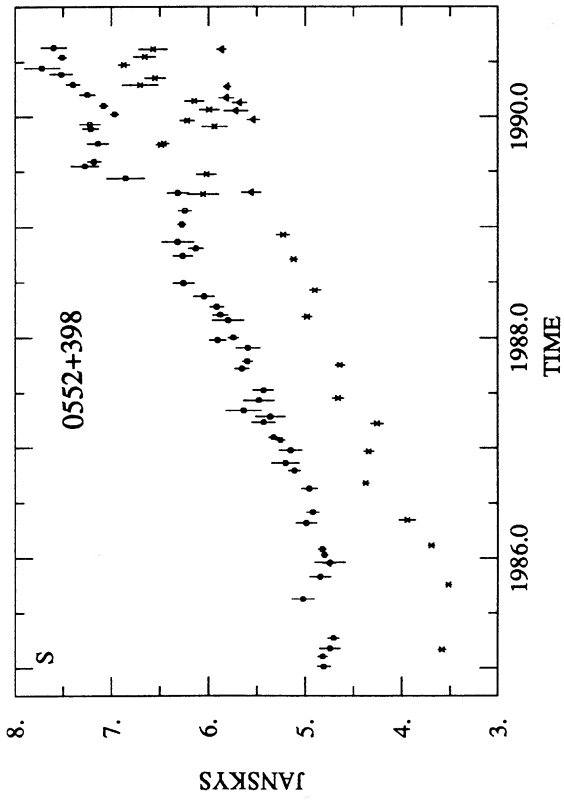


FIG. 1f

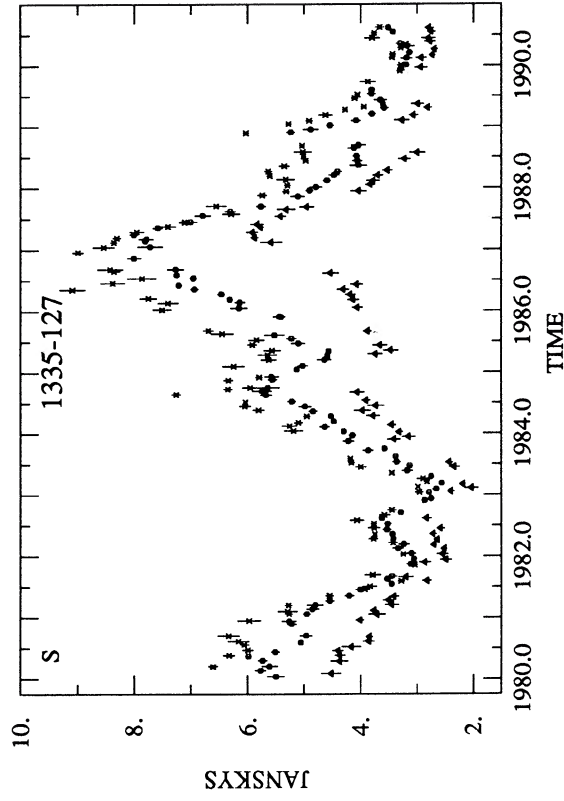


FIG. 1h

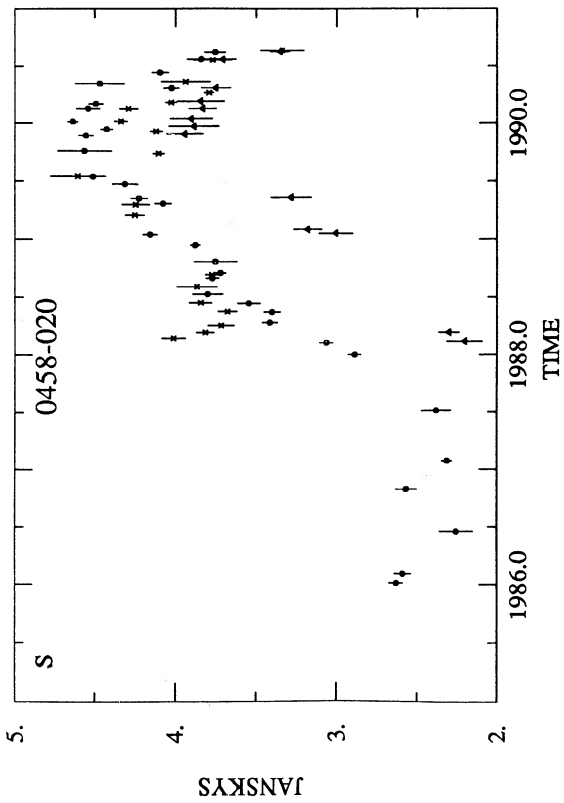


FIG. 1e

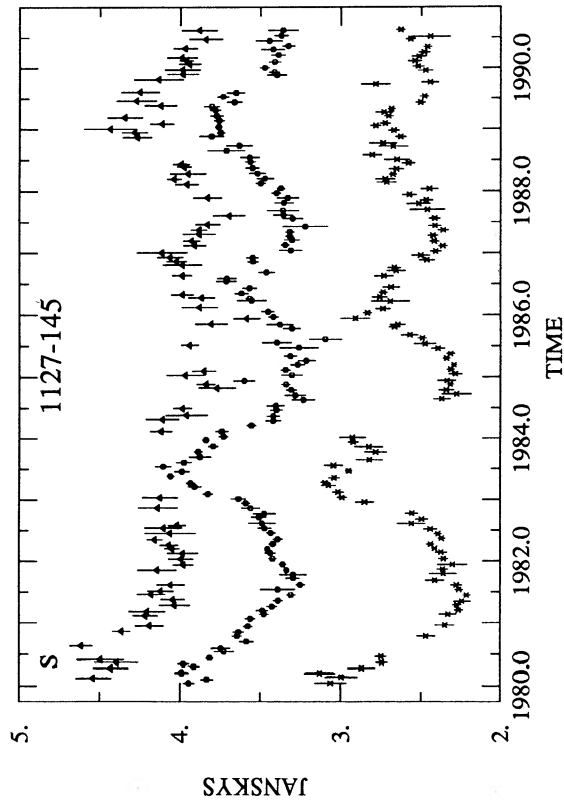


FIG. 1g

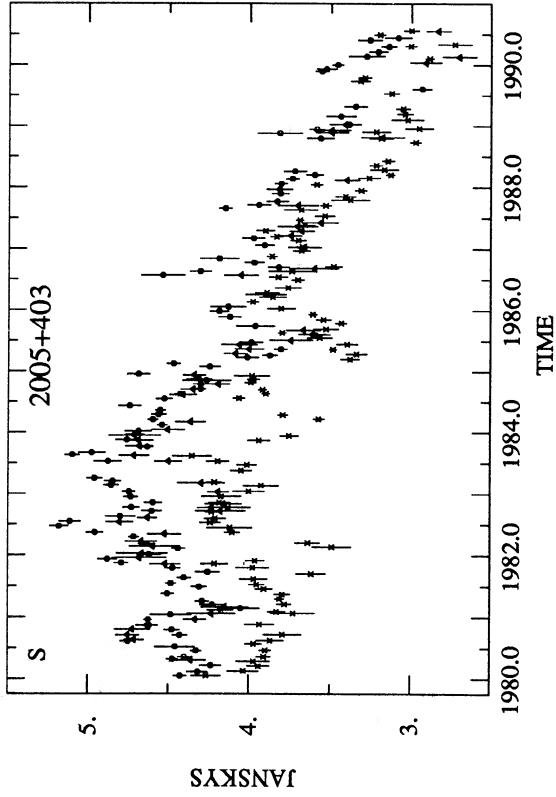


FIG. 1j

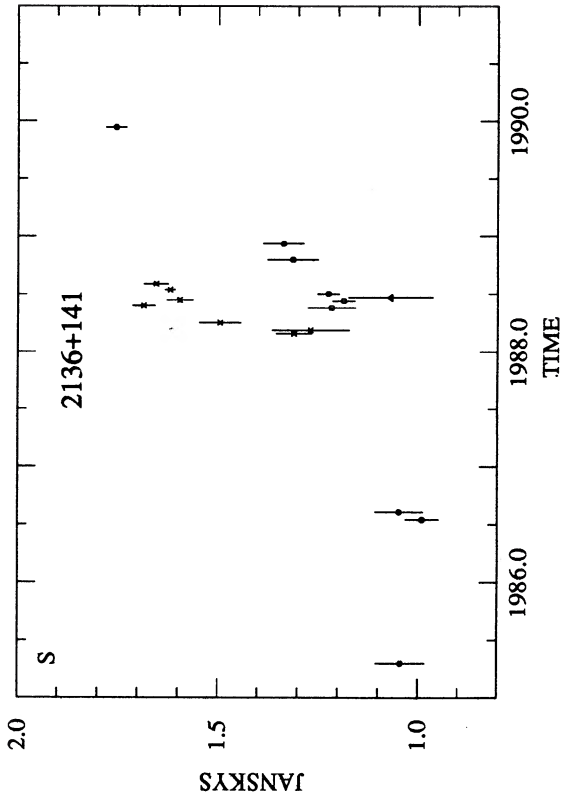


FIG. 1l

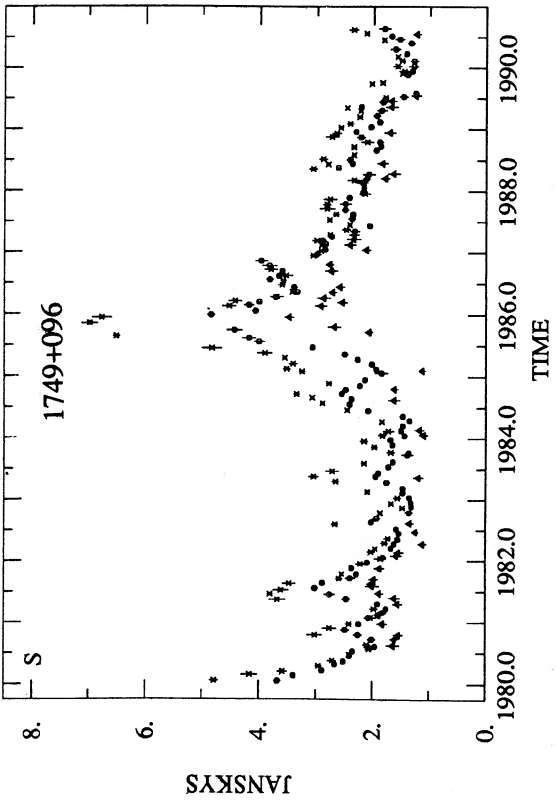


FIG. 1i

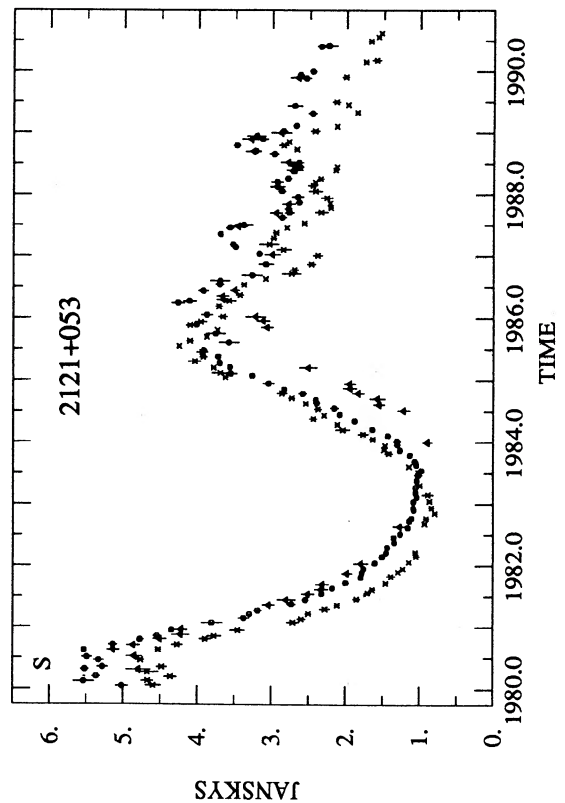


FIG. 1k

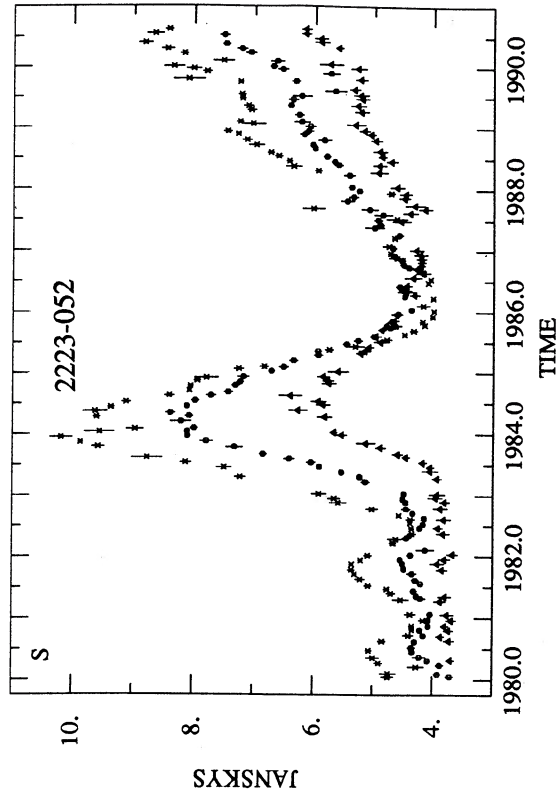


FIG. 1n

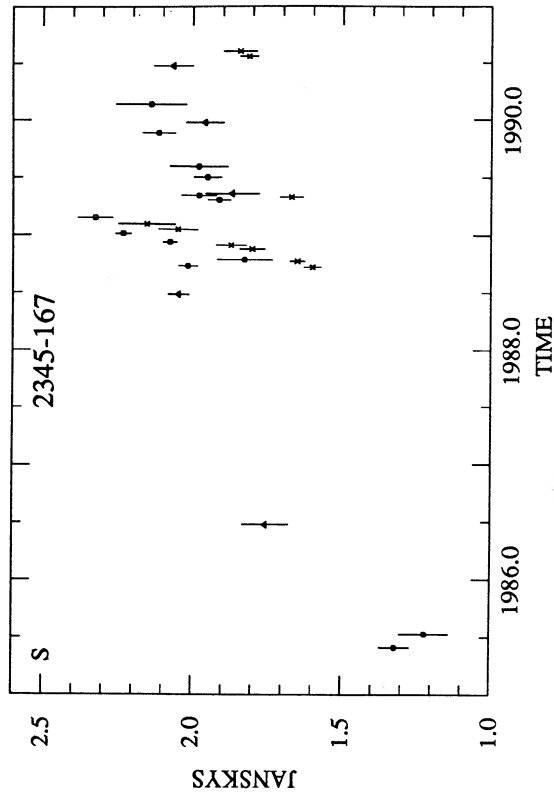


FIG. 1p

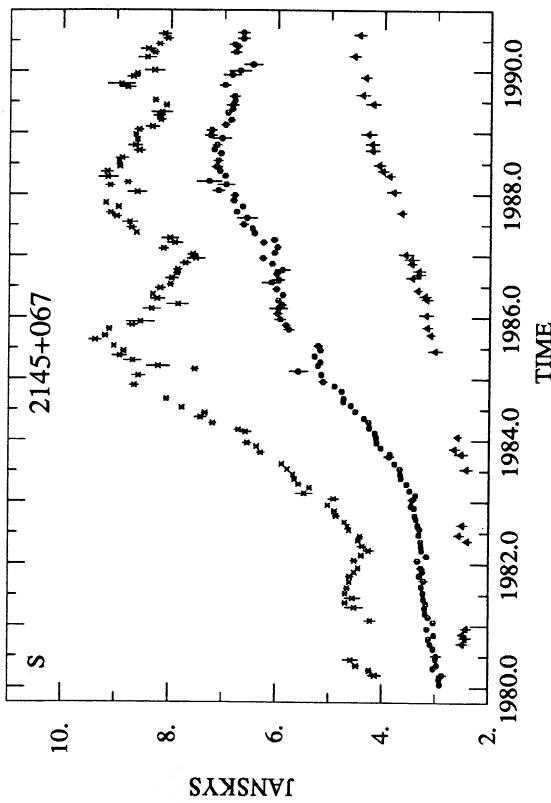


FIG. 1m

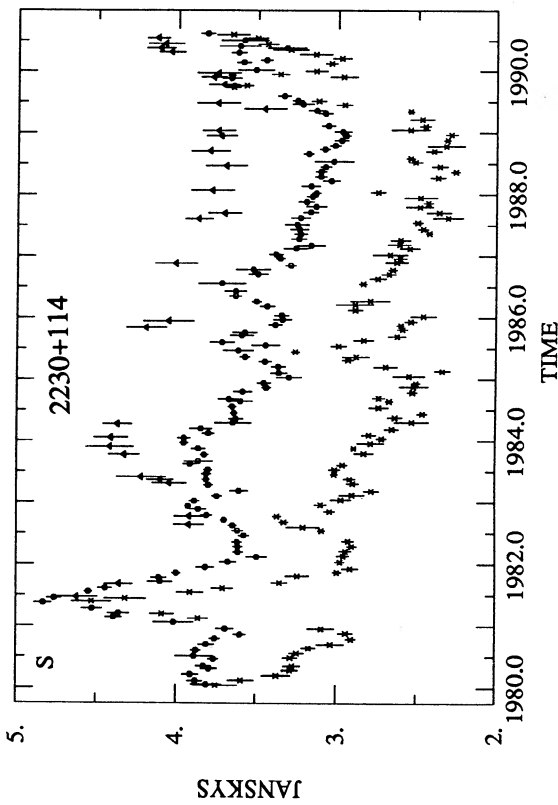


FIG. 1o

TABLE 2
OTHER OBSERVATIONS OF THE VARIABLE SOURCE SAMPLE

Source	Orbiting VLBI	Other VLBI	IRAS (Infrared)	Optical Polarization	EINSTEIN (X-ray)	VLA Map
0234+285.....		L85 M83	N86		O81	R88
0336-019.....	L89			S88	LO85	P82
0420-014.....	L89		N86	S85	O81	P82
0458-020.....		B89		I88	H84	B89
0552+398.....		S83, SE88 C90				P82
1127-145.....	L89	R84, P86		S84	H84	R88
1335+127.....	L89		I84	I88	H84	P82
1749+096.....			I84	K76, W80 S87	LO85	P82
2005+403.....		L85, M90 F89			K80	P82
2121+053.....						P82
2136+141.....		Z84				P82
2145+067.....					J82	P82
2345-167.....	L89	P89	N86	S88	K80, W87	W84, P82 A85

REFERENCES.—(A85) Antonucci & Ulvestad 1985. (B89) Briggs et al. 1989. (C90) Charlot 1989. (F89) Fey, Spangler, & Mutel 1989. (H84) Henriksen, Marshall, & Mushotzky 1984. (I88) Impey & Tapia 1988. (I84) Impey et al. 1984. (J82) Junkkarinen, Marscher, & Burbidge 1982. (K76) Kinman 1976. (K80) Ku, Helfand, & Lucy 1980. (L85) Lawrence et al. 1985. (LO85) Ledden & O'Dell 1985. (L89) Linfield et al. 1989. (M83) Marscher & Broderick 1983. (M90) Mutel & Lestrade 1990. (N86) Neugebauer et al. 1986. (O81) Owen, Helfand, & Spangler 1981. (P86) Padrielli et al. 1986. (P82) Perley 1982. (P89) Preston et al. 1989. (R84) Romney et al. 1984. (R88) Rusk 1988. (S85) Smith et al. 1985. (S87) Smith et al. 1987. (S88) Smith et al. 1988. (SE88) Sovers et al. 1988. (S83) Spangler, Mutel, & Benson 1983. (S84) Stockman, Moore, & Angel 1984. (W84) Wardle, Moore, & Angel 1984. (W80) Wills et al. 1980. (W87) Worrall et al. 1987. (Z84) Zensus et al. 1984.

frequency was 4.991 GHz with a bandwidth of 1.8 MHz. The observations were scheduled as “snapshots,” with three or four scans of duration up to 1 hr on each source, optimized to maximize the u, v -coverage within the allocated observing time. Using Hartesbeesthoek in the Global Array gave us high resolution on sources with low declinations, although this still leaves large gaps in the (u, v) plane, and corresponding high N-S sidelobes in the “dirty beam.” Most antennas were used in each of the three observing sessions. Flux densities were measured by the 40 m antenna at Owens Valley and the 100 m antenna at Effelsberg during each session. In general the

Owens Valley and Effelsberg fluxes agreed to within 5%, but the absolute flux density calibration is uncertain by up to 10%. We cross-correlated the tapes from the antennas on the JPL/Caltech Block II Correlator. The data were then fringe-fitted using software (CALIB; version 15OCT88) from the NRAO AIPS group, and averaged coherently over 60 s. Images were made using standard self-calibration and mapping programs in the Caltech VLBI software package.

In some cases the data on the shortest baselines were not well fit by the clean components in the full resolution images. For these sources, we restricted the solutions in the mapping-

TABLE 3
VLBI OBSERVATIONS

Observatory	Location	Antenna Diameter (m)	Abbreviation	Sessions ^a
Onsala Space Observatory	Onsala, Sweden	26	S	1, 2, 3
Max-Planck-Institut für Radioastronomie	Effelsberg, FRG	100	B	1, 2, 3
Istituto di Radioastronomia	Medicina, Italy	32	L	1, 2, 3
Westerbork Radio Observatory	Netherlands	14 × 25	W	1, 2, 3
Nuffield Radio Astronomy Laboratories	Jodrell Bank, UK	26	J	1, 2, 3
Hartebeesthoek Radio Astronomy Observatory	South Africa	26	E	1, 2, 3
Arecibo Observatory	Puerto Rico	300 ^b	A	1
Haystack Observatory	Westford, MA	37	K	1, 2, 3
Naval Research Laboratory	Maryland Point, MD	26	N	1
National Radio Astronomy Observatory	Green Bank, WV	43	G	1, 2, 3
North Liberty Radio Observatory	Iowa City, IA	26	I	1, 3
George R. Agassiz Station	Fort Davis, TX	26	F	1, 2, 3
National Radio Astronomy Observatory VLBA	Pie Town, NM	25	P	3
National Radio Astronomy Observatory VLA	Socorro, NM	25	Y	1, 2, 3
Owens Valley Radio Observatory	Big Pine, CA	40	O	1, 2, 3
Hat Creek Radio Observatory	Cassel, CA	26	H	1, 2

^a Session 1: mean observing epoch 1986.44; session 2: 1987.40; session 3: 1988.44.

^b Effective diameter with 5 GHz feed approximately 150 m.

self-calibration cycle and fit the longest baselines first, then permitted the fitting of short baselines. This avoids the well-known error whereby large-scale structure tends to get suppressed by the self-calibration step.

We convolved the clean components with an elliptical Gaussian beam with FWHM approximately equal to that of the dirty beam. When an equatorial source is extended east-west the full resolution (0.9 mas) is available without ambiguity. In these cases, tightly restricting the “clean window” enables rapid convergence in the self-calibration-mapping cycle. At low declinations the dirty beam has large N-S side-lobes (> 50%), which means that there is no single “correct” restoring beam. We used a beam size measured from the main lobe of the dirty beam, which allows the possibility of spurious low-level N-S structure; we draw attention below, in the notes on individual sources, to images which require caution in interpretation.

4. IMAGES

The images made from our VLBI observations are shown in Figure 2. The position angle of known large-scale structure, from 5 GHz VLA images, is indicated by a broad arrow. These position angles were measured from the compact core to the most prominent outer peak on the arcsecond scale. The smoothing beams are shown as cross-hatched ellipses (FWHM Gaussian) in the lower left corner of each figure. In most cases we took 1.0 mas as the narrow (E–W) beam size. This is close to the FWHM of the dirty beam, which typically is about 0.9 mas (east-west).

Comments on individual sources follow. In cases where the peak in emission occurs at one end of a linear feature, we refer to the peak as the “core.” It is important to realize that these sources have a wide range of redshift, and the emitted frequencies (corresponding to our observing frequency of 5 GHz) have a correspondingly wide range. Systematic comparisons with other images should be made at the same emitted frequency to avoid complications due to spectral gradients.

0234+285.—Our VLBI image shows a bright southern unresolved component, the “core,” and a curved jet. Additional features at the 1% level are probably artifacts. The curvature may be described as a “bend” or perhaps a “wiggle” but it is also reminiscent of the “kink” seen in 3C 273 (Zensus et al. 1988) where the jet appears to jump sideways and then resume its original position angle. In both 0234+285 and 3C 273 this kink occurs at about 8 pc from the core (projected). 0234+285 is about 3 times more luminous than 3C 273 (at the same emitted wavelength). It will be interesting to see if it has moving components as 3C 273 does and if the kink itself moves.

0336–019.—This is another core-jet source, with diffuse emission fading into the noise toward the east. VLBI observations are difficult due to the low declination.

0420–014.—This source shows an extension to the north which may be an artifact related to the declination and the high side-lobe level. Otherwise, it is barely resolved: the amplitudes are well-fitted by the sum of a 2.3 Jy point source and a concentric circular Gaussian with $S = 2.5$ Jy and FWHM = 0.6 mas. These characterizations are of course smaller than the restoring beam, but they do show that the source is very symmetric and compact, but with a central condensation. Another way of describing the symmetry is with the closure phase, which is zero for an object with a center of symmetry. For 0420–014 the closure phases show a

maximum of 2° excursion from zero. This object and another particularly compact source, 1335–127, are discussed further below.

0458–020.—The source has a core-jet structure, with the jet oriented at PA -55° . The two jet components are located about 2 and 4 mas from the core, and the projected length is about 26 pc. A foreground absorber at $z = 2.04$, thought to be a disk of material in the process of forming a galaxy, is responsible for a strong 21 cm absorption feature (see Briggs et al. 1989). A VLA map published by Briggs et al. shows a 2" jet to the southwest. Their low frequency (608 MHz) VLBI maps show lumpy, complex structure at various position angles. The innermost position angle of the core (inner 10 mas) is about -58° in the Briggs et al. map, close to our 6 cm value.

0552+398.—Our 6 cm images show a core with a western extension about 2.4 mas long (21 pc) which begins at PA 270° and changes to PA 290° about 2 mas from the core. Charlton (1989) finds a similar structure in images made from geodetic data. The two images show the result of convolving the CLEAN components with the “conventional” beam of FWHM equal to 1.9×1.0 mas at PA 13° and with a “super-resolved” beam of FWHM equal to 1.0×0.5 mas at PA 13° . Super-resolved images are useful in showing what the small-scale structure might be, but they are not unique, and must be interpreted with caution.

1127–145.—The source is a nearly equal resolved double, with weak emission to the northeast. The light curves (Fig. 1g) show that it has had a steep spectrum between 5 and 14.5 GHz for the last 10 years. In spectrum and flux variations, and also in structure, it resembles CTA 102 (Wehrle & Cohen 1989). Both may be classed as “compact steep-spectrum” (CSS) quasars; at centimeter wavelengths they have a steep spectrum except possibly during flux outbursts, and nearly all the flux density comes from a region less than an arcsecond in size. A VLA image made at 1375 MHz (Rusk 1988) shows a weak, thin jet extending $30''$ at PA 41° .

Two-epoch VLBI observations of 1127–145 have been published by Romney et al. (1984) and Padrielli et al. (1986) in an 18 cm study of low-frequency variables. The 18 cm maps show east-west structures barely resolved plus an extended component either on the north or south side; the data quality precluded an unambiguous location of the extended flux. We find no evidence of a northern or southern extension in our 6 cm data.

1335–127.—The source is barely resolved by our observations: the data are well-fitted by a single circular Gaussian with flux density 5.4 Jy and FWHM 0.4 mas. The closure phases show a maximum excursion of about 3° from 0° .

1749+096.—This source is a BL Lac object and has one of the lowest redshifts in the sample. It has a strong central peak with extensions to the north. Polarization VLBI has been presented by the Brandeis group (Gabuzda et al. 1989): they observed it with four US stations in 1981 December. Due to poor u, v -coverage, they were only able to say that it was extended toward the east. Changes in polarization and radio flux density have been modelled by Hughes, Aller, & Aller (1989, 1990). Figure 2 shows the 1987 image; the 1986 image is very similar.

2005+403.—(not shown in Fig. 2) This source lies behind the Cygnus Superbubble and is heavily broadened by interstellar scattering. Our results are similar to those of Fey, Spangler, & Mutel (1989, Fig. 1): at 6 cm the source may be roughly represented by a circular Gaussian of FWHM about 3 mas, and the diameter varies approximately as λ^2 .

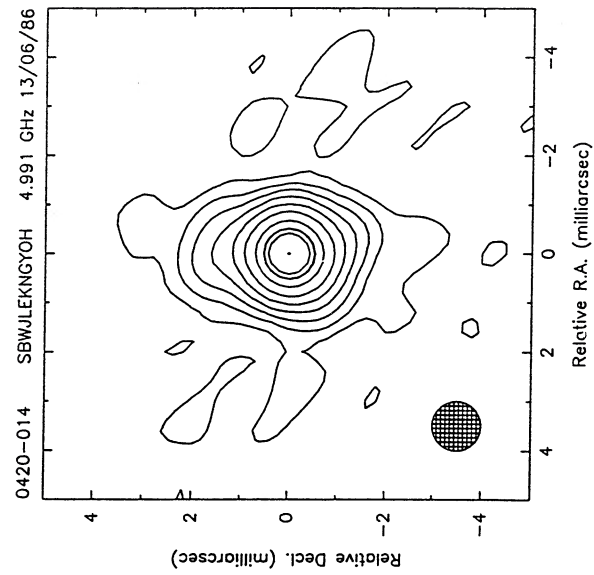


FIG. 2c

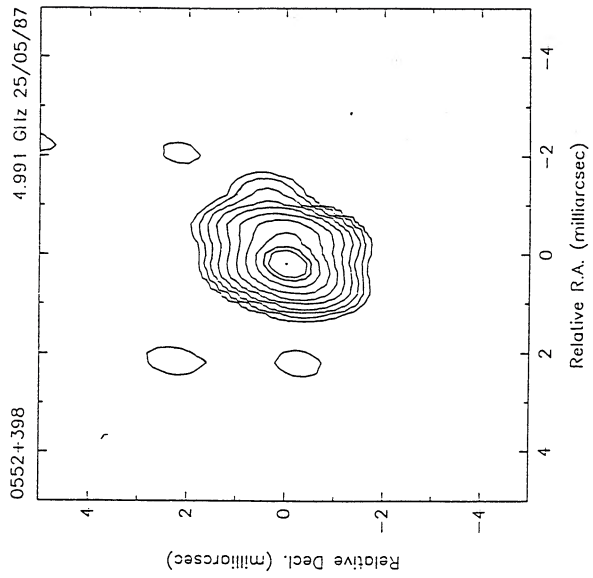


FIG. 2f

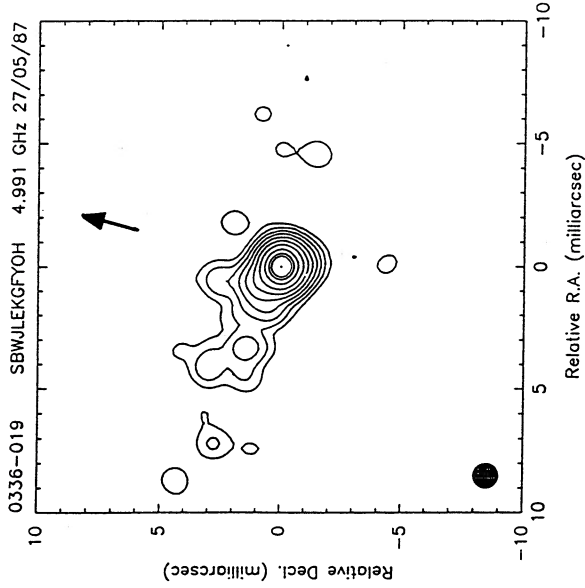


FIG. 2b

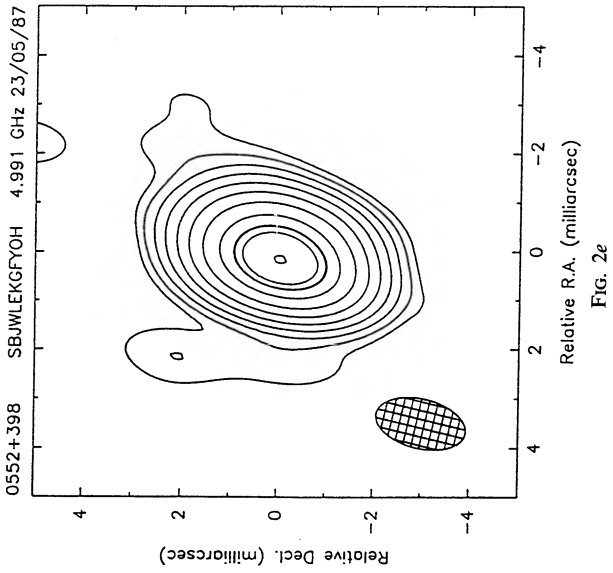


FIG. 2e

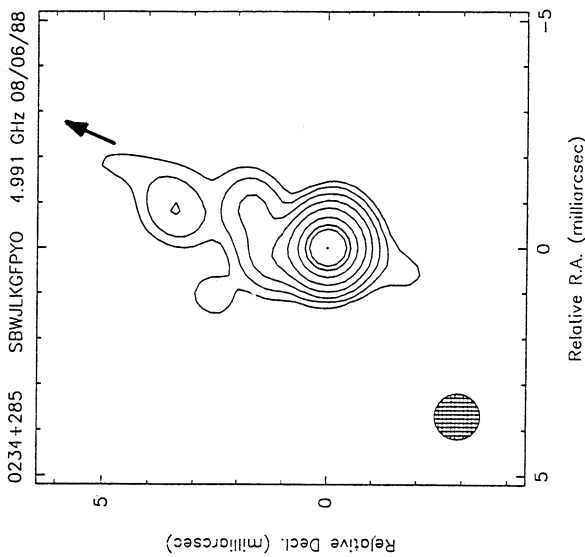


FIG. 2a

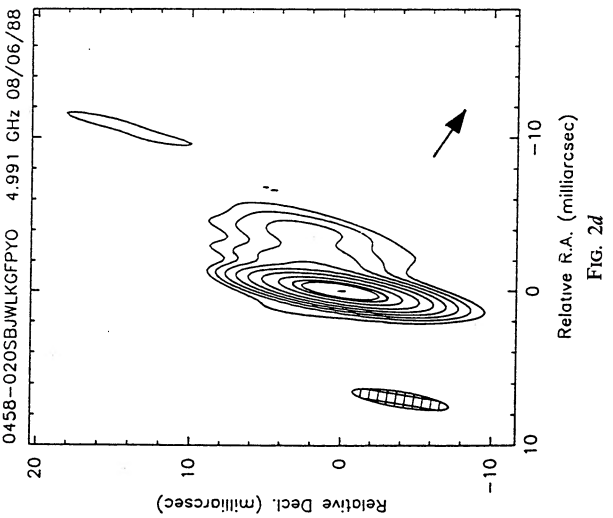


FIG. 2d

FIG. 2.—VLBI images of 12 Variable Source Sample objects and 2136 + 141 at 5 GHz. In addition to full resolution images of 0552 + 398 and 2136 + 141, we show “super-resolved” images to emphasize the bends in the jets. Both full and low-resolution images are shown for 2145 + 067 in order to represent the emission present at various angular scales.

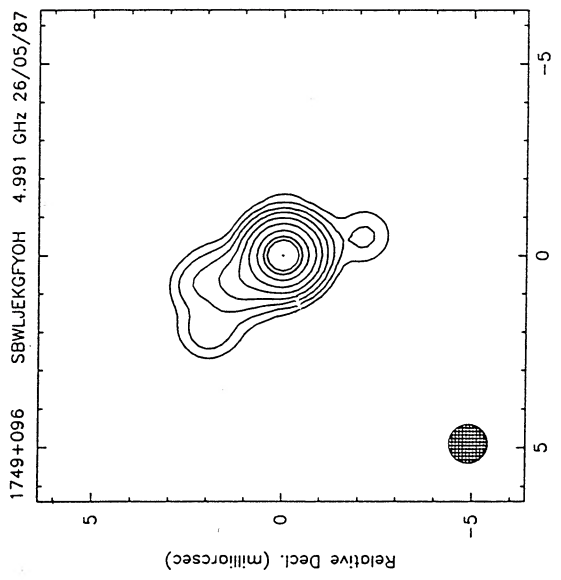


FIG. 2i

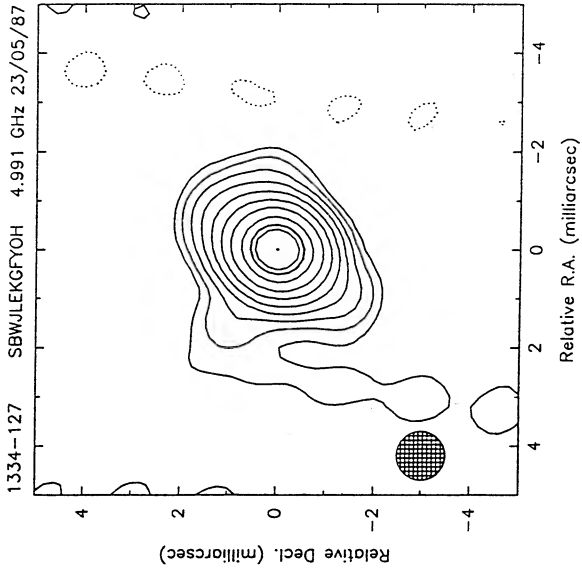


FIG. 2h

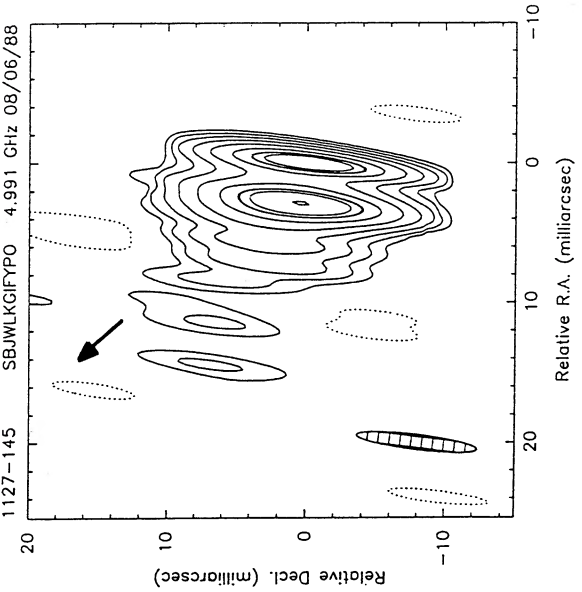


FIG. 2g

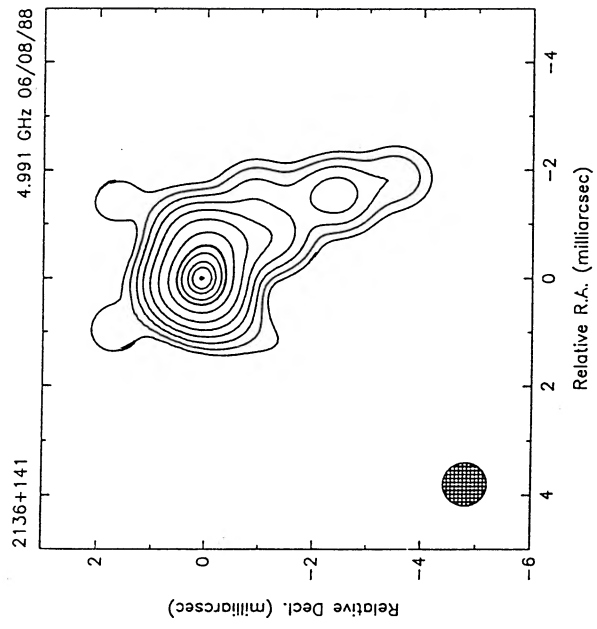


FIG. 2j

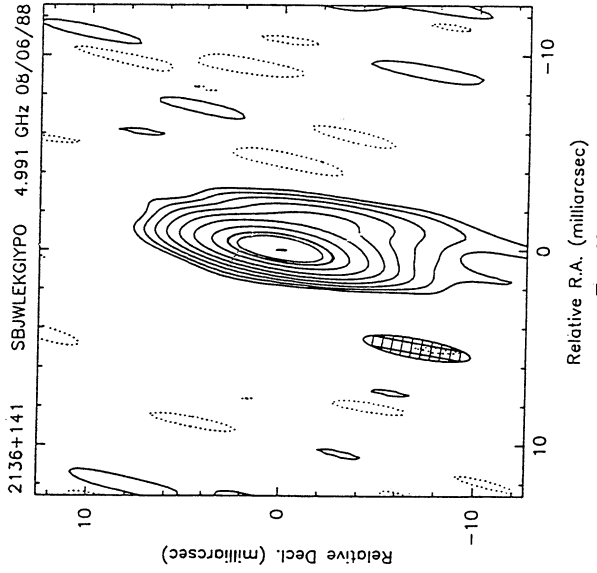


FIG. 2k

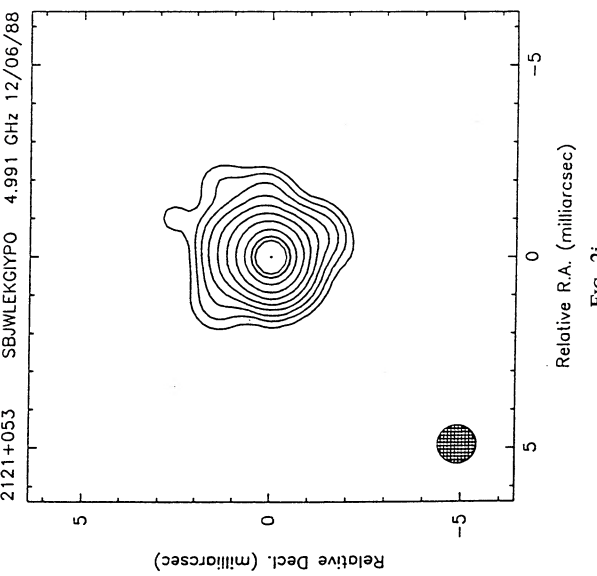
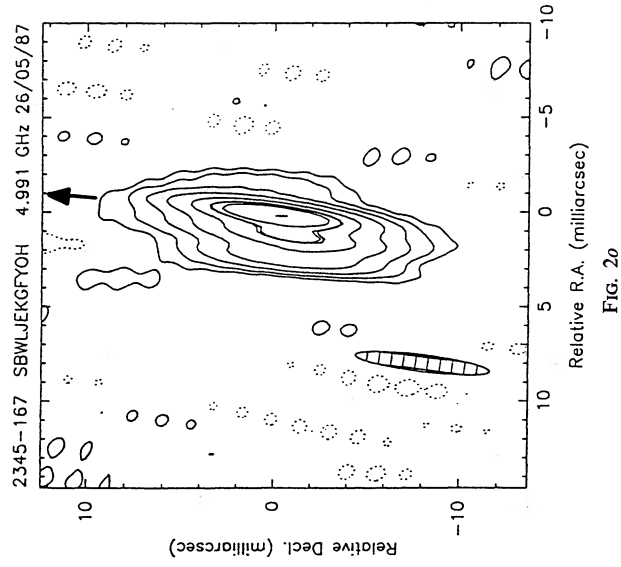
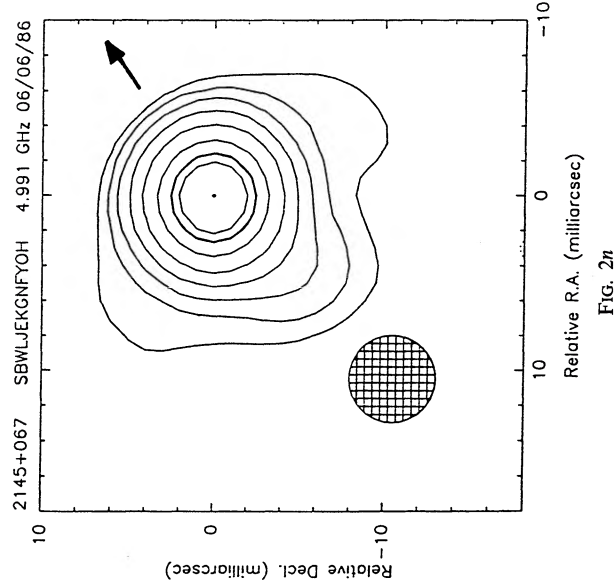
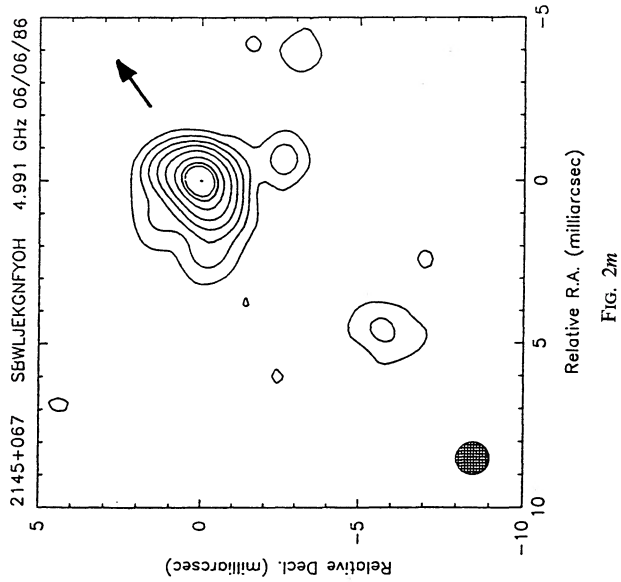


FIG. 2l



2121+053.—This source has a strong peak surrounded by a diffuse halo. A halo on this scale is rare and may not be intrinsic to the source; i.e., it might be caused by interstellar scattering.

Fugmann (1988, 1989) studied the fields around 12 quasars, including 2121+053. He does not quote an individual result for this field, but overall, his results imply that the flux density of 2121+053 may be boosted by gravitational amplification. Crampton et al. (1989) found no evidence for gravitational lensing (multiple images) in 1988 August, when 2121+053 was fairly bright ($M_v = 17.5$).

2136+141.—This source does not meet the flux density criterion for inclusion in the Variable Source Sample, but was included in this series of observations because its high redshift makes any superluminal motion that might be found particularly useful for the μ - z diagram. It has a core-jet structure with at least five components, best seen in the super-resolved image when convolved with a beam with FWHM of 0.8 mas; this image, like all super-resolved images, should be interpreted with caution. The first jet component, about 0.5 mas from the core, is at PA 255°. The jet smoothly turns to PA 210° about 1.2 mas (4.7 pc) from the core and continues to 4.2 mas where it becomes too faint to follow. The bulges to the northeast and northwest of the core at contour level 0.5% are artifacts.

2145+067.—We show two images of this source, because it requires both a full-resolution and a tapered low-resolution image to show the structures present. There is a strong, well-resolved component elongated to the southeast, roughly in the direction of a diffuse component at PA $\sim 140^\circ$. The tapered image (Fig. 2*n*) shows that both components are embedded in a diffuse halo. We are unable to identify a core; neither component is compact, nor do we know which (if either) has a flat spectrum. Perley (1982) found a secondary component at $r = 2''.5$ and PA 305° in his VLA maps. The VLA secondary is almost 180° away from the fainter component in the VLBI image, so if the stronger VLBI component is the core, the jet must bend through 180° between parsec and kiloparsec scales. A complication is added by low-frequency observations: the VLBI structure may be distorted by scattering. The source is variable at low frequencies (Gregorini et al. 1984); but it is not clear if the fluctuations are intrinsic or due to refractive interstellar scintillation (Spangler et al. 1989).

2345-167.—The low-level bulge on the west end is probably an artifact, and we identify the core with the strongest component. A strong secondary, with strength over 50% of the peak, occurs about 1.5 mas from the core at PA 110°. A third component is further to the east at PA 105°. Perley (1982) reports a secondary component at $r = 1''.8$, PA = 355° in VLA maps. If the strongest VLBI component is the core, the jet must bend through about 115° between parsec and kiloparsec scales.

5. SOURCE STRUCTURES

5.1. Comparison with Pearson-Readhead Survey

We compared the morphologies in Figure 2 with those of the Pearson-Readhead (PR88) sources and found no significant differences. Nine of our 13 sources are asymmetric and can be described as “core-jet”; two of the others are very compact (0420-014, 1335-127), one is broadened by interstellar scattering (2005+403), and one is a core-halo (2121+053).

Most of the sources in Figure 2 show nonlinear features, indicating bent jets possibly exaggerated by projection.

None of the 17 sources we have mapped are “compact doubles,” or “compact triples” like 0710+439 and 2352+495 recently mapped by Conway et al. (1990; see also PR88) and it appears that only only of those mapped in the Variable Source Sample is of this category (4C 39.25). These objects tend to be less variable than compact or core-jet objects and thus are less likely to be in the Variable Source Sample.

In compact radio sources, the “core,” when it can be identified, is invariably at one end of the linear structure and is the most compact part of the source at centimeter wavelengths. It has the flattest spectrum and thus represents that portion of the source which persists to the short wavelength (mm) region. However, unlike the sources in the Pearson-Readhead sample, we have found several sources (e.g., CTA 102 and 1127-145) in which the second feature is the brightest at 6 cm. We have presumed that the first feature, not the brightest, is in fact the core. This situation was true of 3C 345 at 6 cm in 1989 (Wehrle & Unwin 1991). At 6 cm a steep-spectrum component can become bright and dominate the source for a period of time. At longer wavelengths the core becomes optically thick and weak, and the steep-spectrum jet components permanently dominate the source.

The Variable Source Sample contains five Compact Steep Spectrum sources: 4C 39.25, 1127-145, 3C 380, 2134+004, and CTA 102. All these objects have two strong components separated by more than one mas, plus a jet or other diffuse emission. This appears to be the clearest association between the spectrum (Fig. 1) and the morphology (Fig. 2) in the Variable Source Sample. Note that the converse is not true; e.g., 3C 345 has on occasion been dominated by two well-separated components and has a jet, but it is not a CSS source. None of these sources shows simple superluminal motion of identifiable features (see references in Table 1).

Pearson & Readhead (1988) defined a morphological class of “very compact” objects, in which the fraction F_c of the total flux which is in the core is greater than 90%. We have two particularly compact and symmetric objects which, although they may not strictly satisfy the Pearson and Readhead criterion, nevertheless deserve special mention. 0420-014 is a tight core-halo with a maximum value of closure phase of two degrees. 1335-127 is barely resolved and can be fit with a single circular component of FWHM 0.4 mas (less than half the beamwidth). Pearson and Readhead had four “very compact” objects out of their flux-limited sample of 65 objects; we have two out of 17 which we have mapped.

These objects may be “naked cores” with little radiation from an extended jet. Alternatively, they could have a radiating straight jet which lies extremely close to the line of sight and which dominates the appearance of maps made with limited dynamic range.

5.2. Comparison of Arcsecond and Milliarcsecond Structures

Pearson & Readhead (1988) examined the difference in position angles, Δ PA, between the orientation of the closest extension to the core on VLBI scales and the orientation of the outer structure as measured at the VLA. They showed, with moderate significance, that Δ PA has peaks at 0° and 90°. We find the same result for the Variable Source Sample; Figure 3 shows the distribution of Δ PA for the objects in the Variable Source Sample which have usable data on both VLBI and VLA scales (measurements on the VLA scale were made from high dynamic range maps in Perley (1982) & Murphy (1988)—almost all Variable Source Sample sources are strongly core-

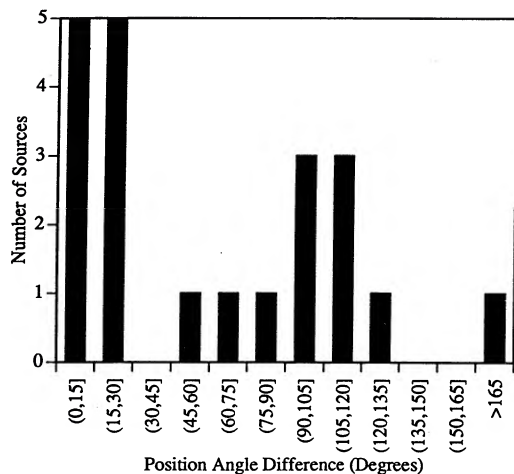


FIG. 3.—Histogram of position angle differences between milliarcsecond and arcsecond scale structures. Objects with differences of about 180° have ambiguous core identifications.

dominated on VLA scales). There is an overlap of only three objects between our Figure 3 and Figure 2 of Pearson & Readhead (1988). The significance of this result, and possible implications are discussed in Wehrle et al. (1992, in preparation).

6. SCALE LENGTHS OF VLBI SOURCES

Radio sources have an enormous range of physical scales; they range from well over a megaparsec for the outer lobes of giant radio galaxies to a parsec or less for the compact objects seen at high resolution. The overall size is intrinsically interesting, but should be studied in conjunction with orientation effects, since most radio objects are elongated. In this study, however, we make no attempt to deproject the sources.

In the discussion below we make use of the measured angular sizes of the Pearson-Readhead and Variable Source Sample sources. We use a “scale length,” similar to *e-folding* length and analogous to the Holmberg radius for galaxies, defined by the extent of a source at 1% of its peak brightness. Like the Holmberg radius for galaxies, defined by the extent of a source at 1% of its peak brightness. Like the Holmberg radius, our “scale length” characterizes the dimensions of an object without regard to its orientation in space: it does not correspond to a particularly significant optical thickness. We first describe the method used to find the angular size, and discuss the reliability of the measurements.

6.1. Angular Size Measurement

We measured angular sizes using the images in Figure 2 for sources we mapped ourselves, and for other sources in the Variable Source Sample and Pearson-Readhead surveys we used the best published VLBI maps (see references in Table 1). On each map we simply took the maximum extent to the lowest reliable contour, then compensated for the convolved source structure by subtracting the (full width) size of the restoring beam at that level. We took the 1% contour on most of our maps as the lowest reliable level. Most other published maps of Variable Source Sample or Pearson-Readhead sources are less reliable, and we used the 5% contour level (if 5% was not plotted, we used the 4% or 6% level). The correct deconvolution depends, of course, on the (unknown) shape of the

underlying source, which is most significant for barely resolved sources (true size less than about half the beam size). We believe, however, that our procedure is approximately correct because (1) most of the sources are elongated with one bright unresolved end; if that end is sharp then the correct procedure is to subtract a half-beamwidth at that end, and (2) the correction at the “jet end” ranges from zero for a long gradually decreasing jet to a half-beamwidth when the jet end also is sharp. We did not attempt to “fine-tune” the corrections for sources individually.

Angular size measurements, hence, scale lengths, are affected to various degrees by the following:

(1) Dynamic range of the image—a weak jet is harder to detect on a poor map and will yield a smaller size than on a good map.

(2) Aperture plane (or u, v) coverage, bandwidth smearing, and averaging effects—VLBI images are usually made from data with a limited range of baseline lengths (typically 100:1 or less). This limits the sensitivity to very extended emission, and hence leads to underestimation of the angular size. The present VLBI observations could have detected bright compact components out to large radii (about 500 mas), but none were found. Our 2 MHz bandwidth did not introduce any significant amount of smearing in the images. Averaging of the visibilities over 60 s would result in about 33% reduction in the flux from a source located 340 beamwidths from the map center, for sources at 90° declination (see eq. [6.71] of Thompson, Moran, & Swenson 1986).

(3) Source morphology—“edge-brightened” objects are easy to measure even with limited dynamic range. Objects with “fuzzy edges” or core-jet sources are more difficult because the angular size depends on the relative prominence of the core. The size of the convolving beam can produce varying results (even after correction) because fainter extended emission may become more visible with a large beam.

(4) Observing frequency—spectral-index differences affect the relative prominence of different source components.

The “corrected” angular sizes shown in Table 4 range from much smaller than a beam (typically 0.9 mas for the present VLBI maps) for slightly resolved sources, to many beamwidths for most objects. The “corrected” angular sizes were converted to linear “sizes” using $H_0 = 100 \text{ km s}^{-1} \text{ Mpc}^{-1}$ and $q_0 = 0.5$. We prefer the term “scale length” to “linear size” because the former emphasizes the uncertainties inherent in the measurements.

6.2. Discussion of scale lengths

Table 4 gives the scale lengths of Variable Source Sample objects. Note that many of our sources have redshifts between 1 and 3, where for a given angular size, the physical scale changes only slowly with redshift (1 mas corresponds to ≈ 4 pc).

The sources for which we have maps have a large range of redshifts, so that images made at one observing frequency are of the source structures at various emitted frequencies. There is insufficient information available to allow extrapolation of various map features to a standard frequency. Generally speaking, cores have flat spectra and jets have steep spectra, so as we move to higher redshifts, the jets will fade faster than the cores. This will tend to make observed sources appear smaller at higher redshifts. A small but opposite tendency may exist due to optical depth effects near the base of the jet (Königl 1981); this has been seen clearly only in 3C 345, where the

TABLE 4
SCALE LENGTHS OF THE SOURCES
A. VARIABLE SOURCE SAMPLE

Source	Redshift	Emitted Wavelength (cm)	Scale $q = 0.05$ (pc mas ⁻¹)	Scale $q = 0.5$ (pc mas ⁻¹)	Size at 1% Contour (mas)	Beam 1% Contour (mas)	Adjusted Size (mas)	Adjusted Size $q = 0.05$ (pc)	Adjusted size $q = 0.5$ (pc)	Notes
0106+013.....	2.017	2.0	6.1	4.1	4.4	2.6	1.8	10.9	7.3	
0133+476.....	0.860	3.2	5.0	4.2	8.6	6.1	2.5	12.5	10.4	5% level
0234+825.....	1.213	2.7	5.6	4.3	7.4	2.6	4.8	26.7	20.7	
0235+164.....	0.940	3.1	5.2	4.2	9.1	9.1	1*	5.2	4.2	unresolved
0316+413.....	0.017	5.9	0.2	0.2	12.6	5.3	7.3	1.8	1.8	5% level
0336-019.....	0.852	3.2	5.0	4.2	5.5	2.6	2.9	14.5	12.1	
0355+508.....										
0420-014.....	0.915	3.1	5.1	4.2	4.0	2.6	1.4	7.2	5.9	
0430+052.....	0.033	5.8	0.5	0.5	55.0	2.6	52.4	24.1	23.6	
0458-020.....	2.286	1.8	6.1	4.0	6.7	2.6	4.1	24.9	16.3	
0528+134.....										
0538+498.....	0.545	3.9								
0552+398.....	2.365	1.8	6.1	3.9	3.4	2.6	0.8	4.9	3.1	
0605-085.....	0.870	6.0								
0607-157.....	0.324	4.5								
0727-115.....										
0735+178.....	0.424	4.2								
0851+202.....	0.306	4.6								
0923+392.....	0.699	3.5	4.7	4.0	6.3	4.6	1.7	7.7	6.7	5% level
1127-145.....	1.187	2.7	5.5	4.3	18.2	2.6	15.6	86.3	67.1	
1226+023.....	0.158	5.2	1.8	1.8	29.4	2.6	26.8	49.3	47.7	
1253-055.....	0.538	3.9	4.1	3.7	12.0	2.6	9.4	38.8	34.4	
1328+307.....	0.846	3.3								
1335-127.....	0.541	3.9	4.1	3.7	4.2	2.6	1.6	6.6	5.9	
1510-089.....	0.361	4.4								
1633+382.....	1.814	2.1	6.0	4.2	4.3	3.8	0.5	3.0	2.1	5% level
1641+399.....	0.595	3.8	4.3	3.8	11.6	2.6	9.0	39.0	34.1	
1730-130.....	0.902	3.2								
1749+096.....	0.321	4.5	3.1	2.9	4.8	2.6	2.2	6.8	6.3	
1828+487.....	0.691	3.5	4.6	4.0	20.6	4.4	16.2	74.8	64.6	5% level
1928+738.....	0.302	6.0	3.0	2.8	10.6	2.5	8.1	23.8	22.5	5% level
2005+403.....	1.736	2.2	5.9	4.2	2.6	2.6	1*	5.9	4.2	unresolved
2121+053.....	1.178	2.8	5.5	4.3	3.5	2.6	0.9	5.0	3.9	
2134+004.....	1.936	2.0	6.0	4.1	4.6	2.6	2.0	12.0	8.2	
2145+067.....	0.990	3.0	5.3	4.3	10.7	2.6	8.1	42.6	34.4	
2200+420.....	0.070	5.6	0.9	0.9	10.9	6.1	4.8	4.4	4.3	5% level
2201+315.....	0.297	4.6								
2223-052.....	1.404	2.5	5.7	4.3	11.6	2.6	9.0	51.6	38.6	
2230+114.....	1.037	2.9	5.3	4.3	23	2.6	20.4	108.7	87.1	
2251+158.....	0.859	3.2	5.0	4.2	12.4	2.6	9.8	49.3	40.9	
2345-167.....	0.600	3.8	4.4	3.8	5.2	2.6	2.6	11.3	9.9	

B. PEARSON-READHEAD SAMPLE

0016+731.....	1.781	2.16	6.0	4.2	4.3	3.8	0.5	3.0	2.1	
0108+388.....					10.3	5.3	5.0			
0133+476.....	0.859	3.23	5.0	4.2	8.6	6.1	2.5	12.5	10.4	
0153+744.....	2.338	1.80	6.1	3.9	12.9	2.7	10.1	61.7	39.5	
0212+735.....	2.367	1.78	6.1	3.9	14.9	2.5	12.3	75.1	48.1	
0316+413.....	0.017	5.90	0.2	0.24	12.6	5.3	7.3	1.8	1.8	
0454+844.....					3.4	2.7	0.7			
0710+439.....	0.518	3.95	4.1	3.6	25.7	2.9	22.8	92.2	82.0	
0711+356.....	1.620	2.29	5.9	4.2	9.1	3.8	5.4	31.5	22.5	
0804+499.....	1.430	2.47	5.8	4.3	2.9	2.7	0.2	1.4	1.0	
0814+425.....					6.7	6.7	1*			unresolved
0831+557.....	0.242	4.83	2.5	2.4	8.1	4.2	3.9	10.0	9.5	
0836+710.....	2.170	1.89	6.1	4	5.4	2.5	2.9	17.6	11.6	
0850+581.....	1.322	2.58	5.7	4.3	7.1	3.2	4.0	22.6	17.2	
0859+470.....	1.462	2.44	5.8	4.3	7.4	6.1	1.3	7.7	5.8	
0906+430.....	0.670	3.59	4.6	3.9	3.7	3.2	0.6	2.6	2.2	
0923+392.....	0.699	3.53	4.7	4	6.3	4.6	1.7	7.7	6.7	
0945+408.....	1.252	2.66	5.6	4.3	9.7	4.4	5.3	29.7	22.8	
1458+718.....	0.905	3.15	5.1	4.2	29.1	2.7	26.4	135.2	110.9	
1624+416.....	2.550	1.69	6.1	3.8	5.7	2.7	3.0	18.2	11.3	
1633+382.....	1.814	2.13	6.0	4.2	4.3	3.8	0.5	3.0	2.1	
1637+574.....	0.745	3.44	4.8	4.1	5.7	5.7	1*	4.8	4.1	unresolved
1642+690.....	0.751	3.43	4.8	4.1	6.0	2.5	3.5	16.6	14.3	
1652+398.....	0.034	5.80	0.5	0.46	5.4	4.0	1.4	0.7	0.7	

TABLE 4—Continued

Source	Redshift	Emitted Wavelength (cm)	Scale $q = 0.05$ (pc mas ⁻¹)	Scale $q = 0.5$ (pc mas ⁻¹)	Size at 1% Contour (mas)	Beam 1% Contour (mas)	Adjusted Size (mas)	Adjusted Size $q = 0.05$ (pc)	Adjusted size $q = 0.5$ (pc)	Notes
1739+522.....	1.375	2.53	5.7	4.3	1.7	1.7	1*	5.7	4.3	unresolved
1749+701.....					3.7	2.3	1.4			
1803+784.....	0.680	3.57	4.6	4	3.4	2.3	1.1	5.1	4.5	
1807+698.....	0.050	5.71	0.7	0.67	17.1	3.6	13.6	9.1	9.1	
1823+568.....	0.664	3.61	4.6	3.9	2.9	2.3	0.5	2.5	2.1	
1828+487.....	0.692	3.55	4.6	4	20.6	4.4	16.2	74.8	64.6	
1845+797.....	0.057	5.68	0.8	0.75	7.7	3.6	4.1	3.1	3.1	
1928+738.....	0.302	4.61	3.0	2.8	10.6	2.5	8.1	23.8	22.5	
1954+513.....	1.220	2.70	5.6	4.3	6.0	5.3	0.8	4.2	3.2	
2021+614.....	0.227	4.89	2.4	2.3	12.0	4.2	7.8	18.9	17.9	
2200+420.....	0.070	5.61	0.9	0.9	10.9	6.1	4.8	4.4	4.3	
2351+456.....	2.000	2.00	6.0	4.1	8.6	6.5	2.1	12.7	8.7	15% level
2352+495.....	0.237	4.85	2.5	2.4	20.1	2.9	17.2	43.0	41.3	

magnitude of the effect is only 0.5 mas between 2.3 and 10.7 GHz (Biretta, Moore, & Cohen 1986).

The projected scale lengths for the Variable Source Sample and Pearson-Readhead samples are shown in Figure 4. There is no obvious relation between scale length and redshift, other than that all the large objects (scale lengths greater than 60 pc) have $z < 1.5$. This may be due to the redshift effect mentioned above, the disappearance of the redshifted jet because of spectral gradients. Alternatively, it could be due to high-redshift objects having higher apparent luminosity on average, which might result from stronger Doppler boosting and thus increased core dominance; or it could be due to increased

interstellar densities which break up or bend the collimated beam more quickly. We draw attention to several sources whose recent high dynamic range VLBI images show fairly well-collimated jets that flare suddenly, either at the "end" of the jet or near a bend in the jet: 3C 345 (Wehrle & Unwin 1991), M87 (Reid et al. 1989), 3C 371 (PR88 and Lind 1987), 0945+408 (PR88 and Conway et al. 1992, in preparation), CTA 102 (Wehrle & Cohen 1989), 3C 380 (Wilkinson et al. 1990) and 3C 309.1 (Wilkinson et al. 1986).

The three largest objects in Table 4 are all CSS quasars. However, the numbers of objects are small. Taken together (Table 5), the five CSS quasars have a mean scale length

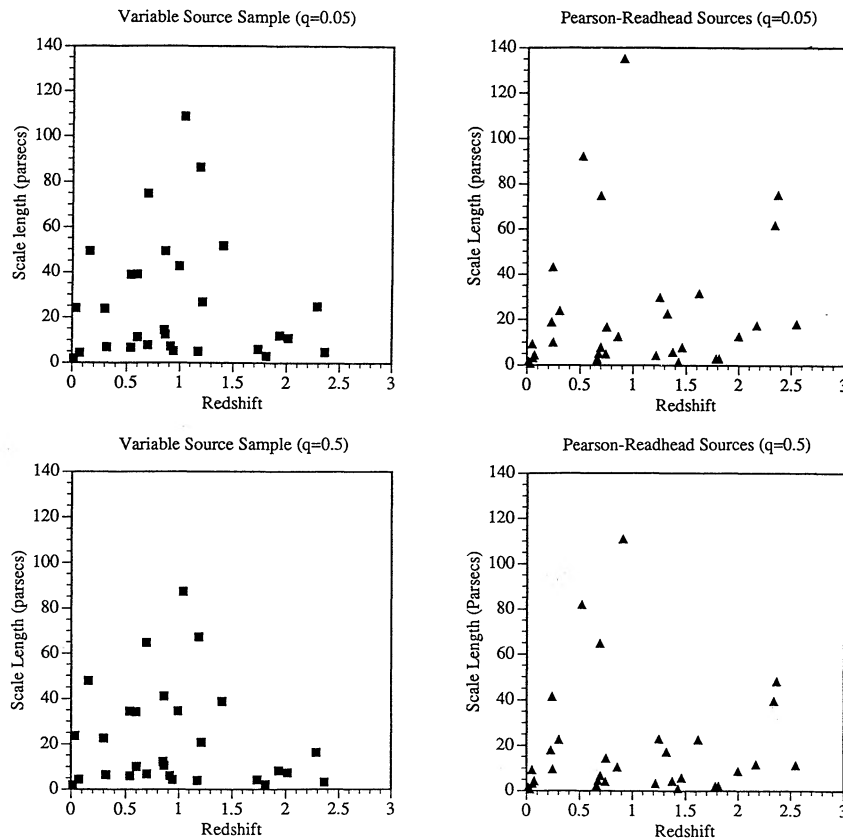


FIG. 4.—Scale lengths of Variable Source Sample and Pearson-Readhead sources as a function of redshift

TABLE 5
SCALE LENGTHS OF COMPACT STEEP-SPECTRUM
QUASARS, FLAT-SPECTRUM QUASARS AND BL LACERTAE OBJECTS
AT REDSHIFTS LESS THAN 1.5

Number of Objects	Object Type	Scale Length (pc)
4.....	Compact steep spectrum Quasars	56 ± 34
13.....	Flat-spectrum quasars	22 ± 15
4.....	BL Lac objects	13 ± 17
3.....	BL Lac objects (excluding 3C 446)	5 ± 1

47 ± 37 pc; the 18 non-CSS (i.e., flat-spectrum) quasars have a mean scale length 18 ± 15 pc; and the four BL Lac objects have a mean scale length 13 ± 17 pc. There are no significant differences in these means. However, to compare objects in the same redshift range, we should examine only $z < 1.5$ since there are no BL Lac objects at larger redshifts; this gives means of 56 ± 34 , 22 ± 15 , and 13 ± 17 pc, for the four CSS quasars, the 13 flat-spectrum quasars, and the BL Lac objects, respectively. Now 3C 446 ($z = 1.404$) is often called a quasar instead of a BL Lac object. This semantic difference is not important since 3C 446 is on the quasar/BL Lac boundary: sometimes it shows emission lines and sometimes it doesn't. In scale length and luminosity, it is more like a quasar than a BL Lac object. If we don't count it at all then the BL Lac mean (three objects) becomes 5 ± 1 pc. Although the numbers are small, it does appear that the CSS quasars are on average larger than flat-spectrum quasars, which are larger than the BL Lac objects. The small scale length for BL Lac objects might indicate that they lie closer to the line of sight, on average than quasars, though Mutel et al. (1990) and others have suggested that they are in fact viewed at larger angles. The lack of long VLBI jets in BL Lac objects might be connected with their lack of strong emission lines. More high-dynamic-range VLBI observations as well as the polarization observations of Gabuzda et al. (1989, 1992) are needed to properly characterize the typical parsec-scale morphology of BL Lac objects.

7. THE RATIO OF X-RAY TO RADIO LUMINOSITIES

The X-ray emission is interesting because it appears that part of it is isotropic and part is beamed inverse-Compton radiation from the radio jet (Worrall & Wilkes 1990, and references therein). In addition, the X-ray properties of a sample can be used to address the question of "unified schemes."

Ledden & O'Dell (1985) showed that BL Lac objects have systematically higher ratios of X-ray to radio luminosity than quasars. We have examined the ratio of relative luminosities in the X-ray and radio spectral bands for the 20 sources in common between the Variable Source Sample and Table 5 in Impey & Neugebauer (1988); we find agreement with Ledden and O'Dell, but note that there is a partial overlap between this sample and ours. Computational details of the relative luminosities in the different spectral energy zones are given in § IVb of Impey & Neugebauer (1988).

The distribution of L_x/L_r is shown in Figure 5, where it can be seen that the BL Lac objects have systematically higher values of L_x/L_r than the quasars. The BL Lac objects in the sample cluster at high values of L_x/L_r (8–33) while the quasars cluster at very low values of L_x/L_r (~ 2) or high values (~ 10); 3C 273 has an exceptionally high value of 59. Only 3C 345 and

3C 273 reach the levels of the BL Lac objects. The low point in Figure 5, $L_x/L_r = 0.4$, is for the lone galaxy, 3C 84. This effect is not due to disparate redshift distributions; the BL Lac objects and quasars have quite similar distributions. Worrall (1989) has reached a similar conclusion in analyzing a blazar sample which overlaps ours somewhat.

Worrall & Wilkes (1990) have suggested that this result can be obtained if the beamed contribution to the X-ray emission (correlated with the radio emission) in BL Lac objects is less important than the isotropic contribution. A reduction in beamed emission might be due to smaller doppler factors in BL Lac objects than in quasars. This qualitatively agrees with the suggestions made (for other reasons) by Cohen (1989) and Mutel et al. (1990) that BL Lac objects have low values of γ . Alternatively, a reduction in Inverse-Compton beamed emission might result from larger emitting regions in BL Lac objects compared to quasars. We do not favor the larger emitting region option for decreasing the X-ray flux because VLBI images show no evidence of larger components or longer relativistic jets in BL Lac objects than in quasars.

Worrall & Wilkes (1990) found another difference between BL Lac objects and core-dominated quasars: the BL Lac objects have X-ray (0.1–3.5 keV) spectral indices which are systematically softer than those of the quasars. These spectral differences suggest that there are intrinsic differences between BL Lac objects and core-dominated quasars, in addition to absolute luminosity, and that they should not be lumped together for statistical purposes (Worrall & Wilkes 1990).

8. THE RELATION BETWEEN LUMINOSITY AND ORIENTATION

The Variable Source Sample objects are variable and core-dominated, and it is likely that most of their cm-wavelength radiation is beamed from a relativistic jet. In this section we investigate the effect the flux-density limit (4.5 Jy at 8 GHz) will have on the possible range of angles and distances of sources in the sample. Specifically, by comparing the (computed) flux of a standard source at various redshifts to the (observed) cutoff flux of our sample, we can establish the orientation angle range or alternatively, we can compute the redshifts at which the standard source would become invisible, i.e., be excluded from the survey, for a range of orientation angles. To investigate the

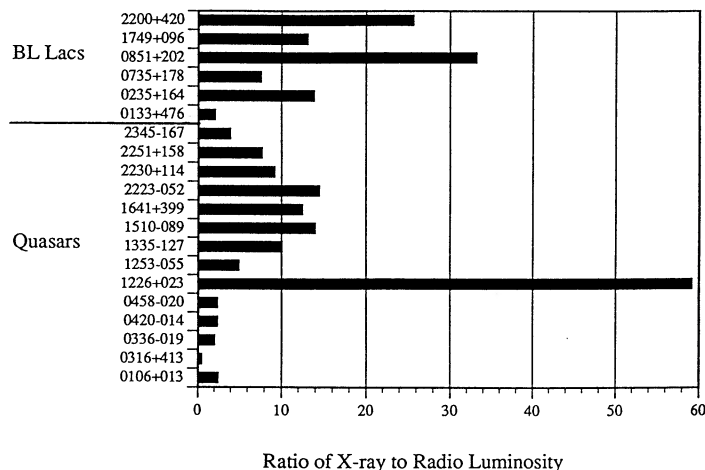


FIG. 5.—Distribution of ratios of $\log L_x/L_r$ for the BL Lacs and quasars in the Variable Source Sample.

likely range of angles we invented a standard source, called 3C 279*, and studied it numerically. This object mimics 3C 279 at its peak flux density: when $z = 0.538$ and $\theta = 1/\gamma$, the flux density is 19.2 Jy at 8 GHz (θ is the angle of the beam to the line of sight). We assumed $\alpha = -0.2$, although the results change slowly with α ; and most importantly, we assumed that 3C 279* has no isotropic flux, i.e., all its radiation comes from a single beam with Lorentz factor γ and small opening angle. We chose 3C 279 for our standard source because it is a very luminous, well-studied object.

We computed the value that θ would have at various redshifts for each of five survey cutoff flux densities, including a low value of $S = 1.125$ Jy which is near the Pearson-Readhead survey limit of 1.3 Jy. The results are shown in Figure 6, which demonstrates that the extreme redshift (for $\theta = 0^\circ$) for 3C 279* to remain in a survey is nearly independent of γ (though it does depend on q_0 for $z > 1$). No source which is intrinsically fainter than 3C 279* will be in the Variable Source Sample if it is located at a redshift greater than 2.85. Using $\alpha = -1.0$ made very little difference—the steep spectrum source disappears at lower redshift ($z = 2.6$ vs. 2.85 for $\theta = 0^\circ$).

Looking in Figure 6 at the $\gamma = 10$ case, for example, we find that the standard source 3C 279* will have $S > 4.5$ Jy at $z = 0.538$ if $\theta < 10^\circ$. If 3C 279* is located at $z = 1$, it must be within 5° to the line of sight to be visible to the survey. If $\gamma = 10$, then the two survey sources at $z > 2$, 0106+013 and 0552+398, must have $\theta < 3^\circ$ and, from Figure 6b, they have $\theta < 9^\circ$ for $\gamma = 3$, if they are as intrinsically luminous as 3C 279*.

Our simulation of 3C 279* demonstrates the highly restricted range of orientation angles for various redshifts and

survey flux cutoffs. Combinations of redshift and orientation which fall to the right of the middle line in Figure 6 place a source in the “zone of invisibility” for our survey (cutoff $S = 4.5$ Jy).

9. SUMMARY

We have defined a new sample, the Variable Source Sample, of 41 core-dominated radio sources chosen on the basis of their peak flux density at any epoch. This list is biased towards highly variable objects. Many of them are already being studied with VLBI, and we show first-epoch VLBI images of 13 of those which have heretofore received little attention.

All sources in the Variable Source Sample are resolved by VLBI observations, although two objects are barely resolved and one is highly scattered by the interstellar medium. The morphologies are similar to those of sources in the statistically-complete Pearson-Readhead survey. Compact steep spectrum objects have larger VLBI scale lengths than flat-spectrum objects or BL Lac objects. Six sources in the Variable Source Sample, all Compact Steep Spectrum sources, have two strong components but are not simple “compact doubles” as characterized by Phillips & Mutel (1982). Most of the Variable Source Sample sources show slightly nonlinear morphologies: the intrinsic bends in the jets are probably amplified by projection effects. We find a striking distribution of position angle differences between large and small-scale radio structures, peaking at 0° and 90° ; this result is discussed separately by Wehrle et al. (1992, in preparation). For sources in the Variable Source Sample, we find that BL Lac objects have a systematically higher ratio of L_x/L_r than the quasars.

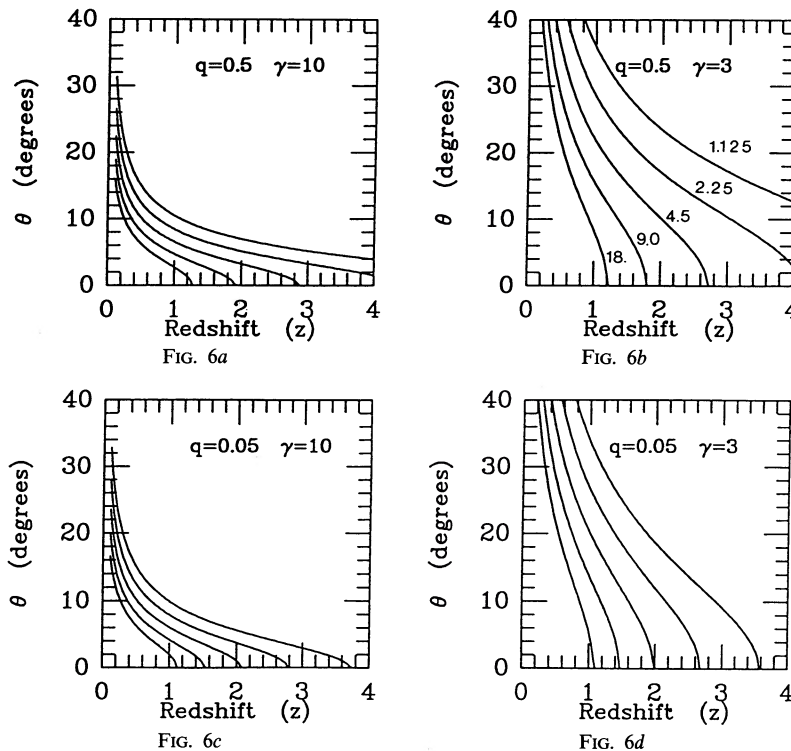


FIG. 6.—Permitted combinations of θ and redshift z for the fiducial source 3C 279* are shown for various values of the cutoff flux density of a survey in Jy (labeled curves). We show the variations for different values of γ and q_0 , since the cosmological distance and amount of beaming are strong determinants of the observed flux density.

Anton Zensus and Peter Barthel contributed to this project in its early stages. We acknowledge useful discussions with René Vermeulen, Alan Marscher, Meg Urry, Diana Worrall, and Sterl Phinney. We are grateful to John Conway and Tim Pearson for showing us VLBI images in advance of publication. We are, as ever, grateful to Tim Pearson for the Caltech VLBI Software Package. Finally, we acknowledge the

dedication of and the years of effort by the Block II team, especially Marty Ewing, Dave Fort, John Peterson, Benho Rayhrer, Dave Rogstad, and Elliot Sigman, which made this research possible. This work was supported at Caltech by grants from the National Science Foundation (AST-85-09822 and AST-88-14544).

REFERENCES

- Alef, W., Preuss, E., Kellermann, K. I., Whyborn, N., & Wilkinson, P. N. 1988, in IAU Symp. 129, *The Impact of VLBI on Astrophysics and Geophysics*, ed. M. J. Reid & J. M. Moran (Dordrecht: Kluwer), 95
- Aller, H. D., Aller, M. F., & Hodge, P. E. 1981, *AJ*, 86, 325
- Aller, H. D., Aller, M. F., Latimer, G. E., & Hodge, P. E. 1985, *ApJS*, 59, 513
- Andrew, B. H., MacLeod, J. M., Harvey, G. A., & Medd, W. J. 1978, *AJ*, 83, 863
- Antonucci, R., & Ulvestad, J. S. 1985, *ApJ*, 294, 158
- Argue, A. N., & Sullivan, C. 1980, *MNRAS*, 192, 779
- Baars, J. W. M., Genzel, R., Pauliny-Toth, I. I. K., & Witzel, A. 1977, *A&A*, 61, 99
- Bääth, L. B. 1984, in IAU Symp. 110, *VLBI and Compact Radio Sources*, ed. R. Fanti, K. Kellermann, & G. Setti (Dordrecht: Reidel), 127
- Biretta, J. A., Moore, R. L., & Cohen, M. H. 1986, *ApJ*, 308, 93
- Bregman, J. N., et al. 1984, *ApJ*, 276, 454
- . 1985, *ApJ*, 291, 505
- Briggs, F. H., Wolfe, A. M., Liszt, H. S., Davis, M. M., & Turner, K. M. 1989, *ApJ*, 341, 650
- Charlot, P. 1989, PhD thesis, L'Observatoire de Paris
- Cohen, M. H. 1989, in *BL Lac Objects* ed. L. Maraschi, T. Maccacaro, & M.-H. Ulrich (Berlin: Springer), 13
- . 1990, in *Parsec-Scale Radio Jets*, ed. J. A. Zensus & T. J. Pearson (Cambridge: Cambridge Univ. Press), 317
- Cohen, M. H., Barthel, P. D., Pearson, T. J., & Zensus, J. A. 1988, *ApJ*, 329, 1
- Condon, J. J. 1988, in *Galactic and Extragalactic Radio Sources*, 2nd ed., ed. G. Verschuur & K. Kellermann (Berlin: Springer), 641
- Conway, J. E., Pearson, T. J., Readhead, A. C. S., & Unwin, S. C. 1990, in *Parsec-Scale Radio Jets*, ed. J. A. Zensus & T. J. Pearson (Cambridge: Cambridge Univ. Press), 167
- Crampton, D., McClure, R. D., Fletcher, J. M., & Hutchings, J. B. 1989, *AJ*, 98, 1188
- Dent, W. A., & Kapitzky, J. E. 1976, *AJ*, 81, 1053
- Eckart, A., Witzel, A., Biermann, P., Johnston, K. J., Simon, R., Schalinski, C., & Kühr, H. 1987, *A&AS*, 67, 121
- Edelson, R. A. 1987, *AJ*, 94, 1150
- Fey, A. L., Spangler, S. R., & Mutel, R. L. 1989, *ApJ*, 337, 730
- Fugmann, W. 1988, *A&A*, 204, 73
- . 1989, *A&A*, 222, 45
- Gabuzda, D. C., Cawthorne, T. V., Roberts, D. H., & Wardle, J. F. C. 1989, *ApJ*, 347, 701
- . 1992, *ApJ*, submitted
- Gregorini, L., Mantovani, F., Eckart, A., Biermann, P., & Witzel, A. 1984, *AJ*, 89, 323
- Henriksen, M. J., Marshall, F. E., & Mushotzky, R. F. 1984, *ApJ*, 284, 491
- Hough, D. H., & Readhead, A. C. S. 1987, *ApJ*, 321, L11
- . 1989, *AJ*, 98, 1208
- Hughes, P. A., Aller, H. D., & Aller, M. F. 1989, *ApJ*, 341, 54
- . 1990, in *Parsec-Scale Radio Jets*, ed. J. A. Zensus & T. J. Pearson (Cambridge: Cambridge Univ. Press), 250
- Impey, C. D., Brand, P. W. J. L., Wolstencroft, R. D., & Williams P. D. 1984, *MNRAS*, 209, 245
- Impey, C. D., & Neugebauer, G. 1988, *AJ*, 95, 307
- Impey, C. D., & Tapia, S. 1988, *ApJ*, 333, 666
- Junkkarinen, V. T., Marscher, A. P., & Burbidge, E. M. 1982, *AJ*, 87, 845
- Kellermann, K., & Owen, F. 1988, in *Galactic and Extragalactic Radio Astronomy*, 2nd ed., ed. G. Verschuur & K. Kellermann (Berlin: Springer), 563
- Kinman, T. D. 1976, *ApJ*, 205, 1
- Königl, A. 1981, *ApJ*, 243, 700
- Ku, W. H.-M., Helfand, D. J., & Lucy, L. B. 1980, *Nature*, 288, 323
- Lawrence, C. R., et al. 1985, *ApJ*, 296, 458
- Ledden, J. E., & O'Dell, S. L. 1985, *ApJ*, 298, 630
- Linfield, R. P., et al. 1989, *ApJ*, 336, 1105
- Lind, K. R. 1987, in *Superluminal Radio Sources*, ed. J. A. Zensus & T. J. Pearson (Cambridge: Cambridge Univ. Press), 180
- Marscher, A. P., & Broderick, J. J. 1983, *AJ*, 88, 759
- Moiseev, I. G., Nesterov, N. S., Efanov, S. V., Strukov, I. A., Korogod, V. V., & Skulachev, D. P. 1988, *Izv. Krym. Astrofiz. Obs.* 78, 112
- Morabito, D. D., Niell, A. E., Preston, R. A., Linfield, R. P., Wehrle, A. E., & Faulkner, J. 1986, *AJ*, 91, 1038
- Murphy, D. W. 1988, PhD thesis, Univ. Manchester
- Mutel, R. L., & Lestrade, J.-F. 1990, *ApJ*, 349, L47
- Mutel, R. L., Phillips, R. B., Su, B., & Bucciferro, R. R. 1990, *ApJ*, 352, 81
- Neugebauer, G., Miley, G. K., Soifer, B. T., & Clegg, P. E. 1986, *ApJ*, 308, 815
- O'Connor, T. 1988, *Users' Guide to the Block II VLBI Correlator*, Jet Propulsion Laboratory, internal document
- . 1989, *Introduction to Block II VLBI Correlator Hardware*, Jet Propulsion Laboratory, internal document
- O'Dea, C. P., Dent, W. A., & Balonek, T. J. 1984, *ApJ*, 278, 89
- Owen, F. N., Helfand, D. J., & Spangler, S. R. 1981, *ApJ*, 250, L55
- Padrielli, L., et al. 1986, *A&A*, 165, 53
- Pauliny-Toth, I. I. K., Porcas, R. W., Zensus, J. A., Kellermann, K. I., Wu, S. Y., Nicolson, G. D., & Mantovani, F. 1987, *Nature*, 328, 778
- Pauliny-Toth, I. I. K., Zensus, J. A., Cohen, M. H., Alberdi, A., & Schaal, R. 1990, in *Parsec-Scale Radio Jets*, ed. J. A. Zensus & T. J. Pearson (Cambridge: Cambridge Univ. Press), 55
- Pearson, T. J., & Readhead, A. C. S. 1988, *ApJ*, 328, 114 (PR88)
- Perley, R. A. 1982, *AJ*, 87, 859
- Phillips, R. B., & Mutel, R. L. 1982, *A&A*, 106, 21
- Preston, R. A., Morabito, D. D., Williams, J. G., Faulkner, J., Jauncey, D. L., & Nicolson, G. D. 1985, *AJ*, 90, 1599
- Preston, R. A., et al. 1989, *AJ*, 98, 1
- Reid, M. J., Biretta, J. A., Junor, W., Muxlow, T. W. B., & Spencer, R. E. 1989, *ApJ*, 336, 112
- Roberts, D. H., Gabuzda, D. G., & Wardle, J. F. C. 1987, *ApJ*, 323, 536
- Romney, J., et al. 1984, *A&A*, 135, 289
- Rusk, R. E. 1988, PhD thesis, Univ. Toronto
- Schalinski, C. J., Alberdi, A., Elósegui, P., & Marcaide, J. M. 1988, in IAU Symp. 129, *The Impact of VLBI on Astrophysics and Geophysics*, ed. M. J. Reid & J. M. Moran (Dordrecht: Kluwer), 39
- Smith, P. S., Balonek, T. J., Elston, R., Heckart, P. A. 1987, *ApJS*, 64, 459
- Smith, P. S., Balonek, T. J., Heckart, P. A., Elston, R., & Schmidt, G. D. 1985, *AJ*, 90, 1184
- Smith, P. S., Elston, R., Berriman, G., Allen, R. G., & Balonek, T. J. 1988, *ApJ*, 326, L39
- Sovers, O. J., Edwards, C. D., Jacobs, C. S., Lanyi, G. E., Liewer, K. M., & Treuhaft, R. N. 1988, *AJ*, 95, 1647
- Spangler, S., Fanti, R., Gregorini, L., & Padrielli, L. 1989, *A&A*, 209, 315
- Spangler, S. R., Mutel, R. L., & Benson, J. M. 1983, *ApJ*, 271, 44
- Steppe, H., Salter, C. J., Chini, R., Kreysa, E., Brunswig, W., & Lobato-Perez, J. 1988, *A&AS*, 75, 317
- Stockman, H. S., Moore, R. L., & Angel, J. R. P. 1984, *ApJ*, 279, 485
- Thompson, A. R., Moran, J. M., & Swenson, G. W., Jr. 1986, in *Interferometry and Synthesis in Radio Astronomy* (New York: Wiley), 177
- Torres, C., & Wroblewski, H. 1987, *A&AS*, 69, 23
- Unwin, S. C., Cohen, M. H., Biretta, J. A., Hodges, M. W., & Zensus, J. A. 1989, *ApJ*, 340, 117
- Valtaoja, E., et al. 1988, *A&A*, 203, 1
- Wardle, J. F. C., Moore, R. L., & Angel, J. R. P. 1984, *ApJ*, 279, 93
- Wehrle, A. E., & Cohen, M. H. 1989, *ApJ*, 346, L69
- Wehrle, A. E., Cohen, M. H., & Unwin, S. C. 1990a, *ApJ*, 351, L1
- . 1990b, in *Parsec-Scale Radio Jets*, ed. J. A. Zensus & T. J. Pearson (Cambridge: Cambridge Univ. Press), 49
- Wehrle, A. E., Morabito, D. D., & Preston, R. A. 1984, *AJ*, 89, 336
- Wehrle, A. E., & Unwin, S. C. 1991, in *Radio Interferometry: Theory, Techniques and Applications*, ed. T. Cornwell & R. Perley (San Francisco: PASP), 354
- Wilkinson, P. N., Kus, A. J., Pearson, T. J., Readhead, A. C. S., & Cornwell, T. J. 1986, in IAU Symp. 119, *Quasars*, ed. G. Swarup & V. K. Kapahi (Dordrecht: Reidel), 165
- Wilkinson, P. N., Tzioumis, A. K., Akujor, C. E., Benson, J. M., Walker, R. C., & Simon, R. S. 1990, in *Parsec-Scale Radio Jets*, ed. J. A. Zensus & T. J. Pearson (Cambridge: Cambridge Univ. Press), 152
- Wills, B. J., & Browne, I. W. A. 1986, *ApJ*, 302, 56
- Wills, D., Will, B. J., Berger, M., & Hsu, Jin-Chung 1980, *AJ*, 85, 1555
- Worrall, D. M. 1989, in *Proc. 23 ESLAB Symp.* (Noordwijk: ESASP-296)
- Worrall, D. M., Giommi, P., Tananbaum, H., & Zamorani, G. 1987, *ApJ*, 313, 596
- Worrall, D. M., & Wilkes, B. J. 1990, *ApJ*, 360, 396
- Zensus, J. A., Porcas, R. W., & Pauliny-Toth, I. I. K. 1984, *A&A*, 133, 27
- Zensus, J. A., Bääth, L. B., Cohen, M. H., & Nicolson, G. D. 1988, *Nature*, 334, 410
- Zensus, J. A., & Porcas, R. W. 1984, in IAU Symp. 110, *VLBI and Compact Radio Sources*, ed. R. Fanti, K. Kellermann, & G. Setti (Dordrecht: Reidel), 163
- . 1987, in *Superluminal Radio Sources*, ed. J. A. Zensus & T. J. Pearson (Cambridge: Cambridge Univ. Press), 126